Published in final edited form as:
J Comp Neurol. 2011 May 1; 519(7): 1301–1319. doi:10.1002/cne.22571.

Forebrain Origins of Glutamatergic Innervation to the Rat Paraventricular Nucleus of the Hypothalamus: Differential Inputs to the Anterior Versus Posterior Subregions

Yvonne M. Ulrich-Lai[1,*], **Kenneth R. Jones**[1], **Dana R. Ziegler**[2], **William E. Cullinan**[2], and **James P. Herman**[1]

[1]Department of Psychiatry, University of Cincinnati, Cincinnati, Ohio 45267

[2]Department of Biomedical Sciences, Marquette University, Milwaukee, Wisconsin 53201

Abstract

The hypothalamic paraventricular nucleus (PVN) regulates numerous homeostatic systems and functions largely under the influence of forebrain inputs. Glutamate is a major neurotransmitter in forebrain, and glutamate neurosignaling in the PVN is known to mediate many of its functions. Previous work showed that vesicular glutamate transporters (VGluTs; specific markers for glutamatergic neurons) are expressed in forebrain sites that project to the PVN; however, the extent of this presumed glutamatergic innervation to the PVN is not clear. In the present study retrograde FluoroGold (FG) labeling of PVN-projecting neurons was combined with in situ hybridization for VGluT1 and VGluT2 mRNAs to identify forebrain regions that provide glutamatergic innervation to the PVN and its immediate surround in rats, with special consideration for the sources to the anterior versus posterior PVN. VGluT1 mRNA colocalization with retrogradely labeled FG neurons was sparse.

VGluT2 mRNA colocalization with FG neurons was most abundant in the ventromedial hypothalamus after anterior PVN FG injections, and in the lateral, posterior, dorsomedial, and ventromedial hypothalamic nuclei after posterior PVN injections. Anterograde tract tracing combined with VGluT2 immunolabeling showed that 1) ventromedial nucleus-derived glutamatergic inputs occur in both the anterior and posterior PVN; 2) posterior nucleus-derived glutamatergic inputs occur predominantly in the posterior PVN; and 3) medial preoptic nucleus-derived inputs to the PVN are not glutamatergic, thereby corroborating the innervation pattern seen with retrograde tracing. The results suggest that PVN subregions are influenced by varying amounts and sources of forebrain glutamatergic regulation, consistent with functional differentiation of glutamate projections.

INDEXING TERMS

vesicular glutamate transporter; FluoroGold; retrograde labeling; *Phaseolus vulgaris* leucoagglutinin; anterograde labeling

The paraventricular nucleus of the hypothalamus (PVN) plays a role in regulating body temperature, sexual function, lactation, food intake, energy balance, water/osmotic balance, and the activities of the hypothalamic–pituitary–adrenocortical axis and the autonomic

[*]CORRESPONDENCE TO: Yvonne M. Ulrich-Lai, PhD, University of Cincinnati, Dept. of Psychiatry-North, 2170 East Galbraith Rd., Reading, OH 45237-0506. yvonne.ulrich-lai@uc.edu.

nervous system (Bisset and Chowdrey, 1988; McKenna, 2001; Nagy et al., 2005; Schlenker, 2005). The PVN is under the control of forebrain/limbic inputs (Herman et al., 2003; Fehm et al., 2006; Lechan and Fekete, 2006), many of which use glutamate as the principal excitatory neurotransmitter. The PVN is heavily innervated by glutamatergic fibers (van den Pol, 1991; Wittmann et al., 2005; Ziegler et al., 2005) and PVN neurons express several types of glutamate receptors (Aubry et al., 1996; Mateos et al., 1998; Herman et al., 2000; Eyigor et al., 2005; Ziegler et al., 2005), suggesting that glutamate is an important neurotransmitter in this region. A prominent role for glutamate signaling in the PVN is supported by studies indicating excitatory effects of glutamate on hypothalamic–pituitary–adrenocortical axis activity (Ziegler and Herman, 2000), sympathetic tone (Badoer et al., 2003; Freeman and Brooks, 2007), sexual behavior (Melis et al., 2004), suckling-induced prolactin release (Nagy et al., 2005), and food intake (Hettes et al., 2003). Collectively, this work suggests that glutamatergic inputs from the forebrain are critical regulators of PVN functions.

The specific forebrain origins of glutamatergic innervation to the PVN are not clear. Interpretation of previous work addressing this question is made difficult by the paucity of specific markers for glutamatergic neurons (e.g., all cells contain some glutamate as a part of normal cellular metabolism). Definitive identification of glutamate neurons has only become possible with the recent cloning of vesicular glutamate transporters, which specifically package glutamate into synaptic vesicles.

Therefore, the present work combines tract tracing with phenotypic markers of glutamate neurons to determine glutamate inputs to the PVN. The retrograde tracing approach uses expression of vesicular glutamate transporter 1 (VGluT1) and 2 (VGluT2) mRNAs as specific markers of glutamatergic neurons (reviewed in Ziegler et al., 2002; Takamori, 2006) combined with retrograde FluoroGold (FG) labeling of PVN-projecting neurons to identify forebrain regions that provide glutamatergic innervation to the PVN and its surround, with special consideration for the sources of innervation to the anterior versus posterior PVN. Given the paucity of VGluT1 mRNA expression in forebrain regions that project directly to the PVN (Kaneko and Fujiyama, 2002; Ziegler et al., 2002; Collin et al., 2003), we hypothesized that PVN-projecting glutamatergic neurons would be characterized primarily by the expression of VGluT2 mRNA. Moreover, we hypothesized that established PVN-projecting forebrain sites with known expression of VGluT2 mRNA (Ziegler et al., 2002; Collin et al., 2003; Lin et al., 2003), such as the ventromedial hypothalamic nucleus, dorsomedial hypothalamic nucleus, lateral hypothalamic area, and posterior hypothalamus nucleus, would be the primary sources of glutamatergic innervation to the PVN. In addition, to corroborate projections identified by retrograde tracing studies, anterograde tracing with *Phaseolus vulgaris* leucoagglutinin (PhaL) was combined with immunolabeling for VGluT2 to determine the extent to which various regions provide glutamatergic inputs to the PVN.

MATERIALS AND METHODS

Experimental animals

Adult, male, Sprague–Dawley rats (250–350 g; Harlan, Indianapolis, IN) were used. Rats arrived at least 1 week prior to the onset of experiments and were housed on a 12-hour light/dark cycle (06:00–18:00) with ad libitum access to normal rat chow and water in a constant temperature-humidity vivarium. All procedures were approved by the University of Cincinnati Animal Care and Use Committee.

FluoroGold injections

Experiments used retrograde labeling of FG targeted to the PVN to identify PVN-projecting neurons. Rats were anesthetized (intraperitoneally [i.p.]) with a mixture of ketamine (95 mg/ kg body weight) and xylazine (12.5 mg/ kg body weight) and then placed into a Kopf (Tujunga, CA) stereotaxic apparatus. Surgical procedures employed aseptic technique. FG (2% in saline vehicle; Fluorochrome, Denver, CO) was backfilled into a glass micropipette with a tip diameter of 10–15 μm. The micropipette was slowly inserted unilaterally into the PVN (from bregma AP −1.5 mm, ML −0.4 mm, and DV −6.65 mm from dura). FG was iontophoretically injected using an intermittent current (2–4 μA with 7 seconds on/off for ≈30 seconds). The micropipette was then slowly raised, the skull hole was filled with bone wax, and the skin incision was wound-clipped.

Following ≈7–10 days recovery, rats were given sodium pentobarbital overdose (150 mg/kg body weight) and perfused with 4% paraformaldehyde in sodium phosphate-buffered saline (NaPBS, 0.1 M, pH 7.4). The brains were removed and placed in vials with 4% paraformaldehyde in PBS overnight, followed by placement into 30% sucrose at 4°C. Coronal microtome sections (25 μm thick) were cut through the brain, placed into cryoprotective solution (30% sucrose, w/v; 1% polyvinlypyrrolidone [PVP-40], w/v; 30% ethylene glycol, v/v; in 50 mM sodium phosphate buffer, pH 7.4), and were stored at −20°C until use.

Preparation of vesicular glutamate transporter cRNA probes

In situ hybridization for VGluT1 and VGluT2 mRNAs was used to specifically identify these two classes of glutamatergic neurons (Ziegler et al., 2002). Antisense cRNA probes complementary to VGluT1 (1666–1976 bp of Access no. NM_053859.1) and VGluT2 (1972–2437 bp of Access. no. NM_053427.1) were generated by in vitro transcription using ^{35}S-UTP, as described previously (Ziegler et al., 2002). The VGluT1 and VGluT2 fragments were each cloned into a pGEM-T Easy plasmid vector, linearized with PvuII (VGluT1) or StyI (VGluT2), and transcribed with T7 (VGluT1) or SP6 (VGluT2) RNA polymerases.

In situ hybridization combined with FG immunocytochemistry

Prior to hybridization, a 1-in-6 series of sections was washed with 50 mM NaPBS and incubated in blocking buffer (0.3% TX-100 and 0.2% bovine serum albumin [BSA] in NaPBS). Sections were hybridized overnight at 45°C with 4.5 × 10^6 cpm ^{35}S labeled probe/ 5 mL/well, diluted in hybridization medium (50% formamide, 20 mM Tris-HCl, pH 7.5, 1 mM EDTA, 335 mM sodium chloride, 1 × Denhardt's, 200 μg/mL salmon sperm DNA, 25 μg/ mL yeast tRNA, 20 mM dithiothreitol, and 10% dextran sulfate). Tissue sections were then rinsed in 2× SSC buffer (1 × SSC = 0.25 M sodium chloride, 0.015 M sodium citrate, pH 7.2) and treated with RNAse A (200 μg/ mL) for 3 hours at 37°C. Sections were washed in 2× SSC, 1× SSC, and 0.5 × SSC at room temperature and incubated for 1 hour at 45°C in 0.5× SSC. Following incubation in blocking buffer at room temperature, the sections were placed into primary antibody directed against FG (1:5,000 in blocking buffer; kindly provided by Dr. Stanley Watson, University of Michigan; Table 1) overnight at 4°C. The sections were washed with 50 mM potassium phosphate buffered saline (KPBS), 0.02% TX-100, and then incubated with affinity-purified biotinylated anti-rabbit immunoglobulin G (IgG) made in goat (1:500 in 50 mM KPBS, 0.02% TX-100; Vector Laboratories, Burlingame, CA). After incubation the sections were washed in 50 mM KPBS, 0.02% TX-100, and incubated in Vectastain ABC Solution (1:1,000 in 50 mM KPBS, 0.1% BSA; Vector Laboratories). After incubation the sections were washed in 50 mM KPBS/0.02% TX-100 and visualized by exposure to 3,3'-diaminobenzidine (DAB; 0.4 mg/mL in 50 mM KPBS/0.005% hydrogen peroxide). FG was visualized by chromagen reaction to provide a

stable signal for detection of colocalization in emulsion-dipped sections. Following rinsing the sections were mounted onto glass slides that were subsequently coated with Kodak photographic emulsion NTB2 (diluted 1:1 with water), air-dried, and stored at 4°C in a light- and humid-free environment for 4 weeks. Following development in Kodak D-19 developer and Rapid Fix solutions, emulsion-dipped sections were dehydrated through a series of graded ethanol, cleared with xylene, and coverslipped using DPX mountant (Fluka, Milwaukee, WI).

PhaL injections and immunohistochemistry

Iontophoretic injection of the anterograde tract tracer PhaL into the ventromedial, posterior, and medial preoptic hypothalamic nuclei, with subsequent visualization of boutons coimmunolabeled for PhaL and VGluT2 in the PVN, was employed to independently determine whether the PVN receives differential VGluT2-positive innervation from these regions along its rostral-caudal extent. Injections of PhaL (2.5% in 10 mM phosphate buffer, pH 8.0; Vector Laboratories) were performed as described above for FG with the following exceptions. First, the unilateral injections were targeted to either the ventromedial nucleus (from bregma AP −2.6 mm, ML 0.6 mm, and DV −9.0 to −9.4 mm from dura), the posterior nucleus (from bregma AP −3.8 mm, ML 0.5 mm, and DV −7.3 to −*7.7* mm from dura), or the medial preoptic nucleus (from bregma AP−0.8 mm, ML 0.45 mm, and DV −8.4 to −8.8 mm from dura). Second, the micropipette tip had a diameter of 20–25 μm and the PhaL was injected using a 5 μA intermittent current (*7* seconds on/off) for 15 minutes.

Following 7–10 days recovery the rats were perfused and the brains were collected and sectioned as described above. For single immunolabeling of PhaL, tissue sections were rinsed in KPBS, incubated in 1% hydrogen peroxide (10 minutes), rinsed, and then incubated in blocking buffer (50 mM KPBS, 0.1% BSA, and 0.2% TX-100) for 1 hour at room temperature. Sections were placed into goat anti-PhaL primary antibody (1:3,000 in blocking buffer; Vector Laboratories; product #AS-2224, lot #N0712) overnight at 4°C. Following incubation the sections were rinsed and placed into affinity-purified biotinylated horse antigoat IgG (1:500 in 50 mM KPBS/0.01% BSA; Vector Laboratories) for 1 hour. Sections were rinsed again and placed into Vectastain ABC Solution (1:1,000 in 50 mM KPBS/0.1% BSA; Vector Laboratories) for 1 hour. After rinsing, sections were stained with DAB (as described above), rinsed, mounted onto slides, dehydrated through a graded series of ethanol, cleared with xylene, and coverslipped with DPX mountant. Dual immunolabeling of PhaL and VGluT2 was performed as described above, except 1) rabbit anti-VGluT2 antibody (1:500; Synaptic Systems, Gottingen, Germany, product #135 402, lot 135402/12) was added to the anti-PhaL primary antibody incubation; and 2) immunolabeling was visualized using Alexa488-conjugated donkey antigoat IgG (1:500; Invitrogen, La Jolla, CA; product #A11055, lot 645148) and Cy3-conjugated affinity purified donkey antirabbit IgG (1:500; Jackson ImmunoResearch Labs, West Grove, PA; product #711-165-152, lot 88464).

Antibody characterization

The anti-FG primary antiserum was generated against the FG molecule. The efficacy of the FG antiserum was verified by dual fluorescence imaging, demonstrating complete overlap between native FG fluorescence and immunofluorescence following incubation of sections with anti-FG.

The specificity of the PhaL immunolabeling was verified by a lack of labeling 1) with omission of the primary antibody; 2) with preabsorption of the primary antibody with PhaL; and 3) in tissues that had not been injected with PhaL.

The anti-VGluT2 primary antiserum recognizes a single 65-kDA band in brain tissue corresponding to the molecular weight predicted for VGluT2, and VGluT2 labeling is lost following omission of the primary antiserum or preabsorption of the antiserum with the immunizing peptide (Zhou et al., 2007; Graziano et al., 2008). VGluT2 immunoreactivity was specifically localized in brain regions known to receive projections from areas containing dense VGluT2 mRNA expression, and the labeling did not correspond with patterns of staining seen using antibodies against VGluT1 (Flak et al., 2009).

Image analysis

Anatomical regions of interest were defined using the Paxinos and Watson (1998) and Swanson (1998) rat brain atlases. Anatomical mapping was performed by viewing material under both brightfield and darkfield microscopy to define anatomical landmarks, including 1) the location and size of the white matter tracts (e.g., fornix, optic tract, etc.) and ventricles; 2) variations in cellular density (e.g., compact zone of dorsomedial hypothalamic nucleus); and 3) variations in the density of VGluT mRNA labeling (e.g., VGluT2 mRNA in the ventromedial hypothalamus). For the bed nucleus of the stria terminalis, the anterodorsal subdivision refers to the entire portion that is dorsal to the crossing of the anterior commissure at that rostral-caudal level, whereas the anteroventral subdivision refers to the entire portion that is ventral to the crossing of the anterior commissure at that rostral-caudal level. Sections were imaged using either an Axioplan 2 microscope (Zeiss, Thornwood, NY) equipped with an imaging system (Axiocam camera and AxioVision release 4.4 software; Zeiss) or an AxioImager.Z1 microscope (Zeiss) equipped with apotome (z-stack) imaging capability (Axiocam MRm camera and AxioVision Release 4.6 software; Zeiss).

Cell counts were performed for the identified anatomical regions at all rostral-caudal levels as they appeared in the evenly spaced, 1-in-6 series of tissue sections. The reported cell counts were not corrected for sampling interval. Since the FG injection sites included different proportions of the PVN, the location of the retrogradely labeled neurons varied across the individual cases. In addition, retrogradely labeled cells varied widely in size, shape, and distribution, making it impossible to generate valid estimates of the mean cell diameter. Hence, uncorrected raw profile counts for individual animals are given, without an attempt to correct them for cell size. We recognize that the larger cells will be somewhat overrepresented in these samples. Criterion for identification of FG-immunoreactive cells was a clearly visible DAB reaction product in the shape of a neuronal cell body, often including neuronal processes. Dual-labeled cells were defined as FG-immunoreactive cells overlain by grain densities 5 times that of an equivalent background area (i.e., an adjacent region containing fiber tracts). The number of cells positive for FG only (DAB-positive) and those doublepositive for FG and VGluT mRNA were counted throughout forebrain. Subsequent analyses focused on brain regions that consistently contained at least 10 FG-positive cells from either the anterior PVN, posterior PVN, or both, reasoning that these brain regions likely represent the primary sources of significant glutamatergic innervation to the PVN and its surround. For the PhaL anterograde analysis, dual fluorescence immunolabeling was imaged throughout the rostral-caudal extent of the PVN via apotome z-stack images (each optical section of z-stack had a thickness of ≈0.45μm) and the relative prevalence of dual-labeled boutons was noted. For clarity of presentation (Figs. 1, 2, 4–6), image contrast and brightness were adjusted using Adobe Photoshop 7.0 (San Jose, CA). In addition, the dodge and burn tools in Adobe Photoshop 7.0 were used in some of the low-magnification brightfield images (Figs. 4–6) to correct for uneven illumination.

RESULTS

FG injection sites and forebrain retrograde labeling

There were six cases in which the FG injection involved the PVN with minimal spread into adjacent structures; these cases varied in the degree of rostral-to-caudal involvement of the PVN (Fig. 1). The FG injection in case 90 included most of the anterior PVN (e.g., bregma −1.4 mm) with a small amount in the dorsal-most portion of the PVN at more caudal levels. Adjacent structures that contained some FG included the peri-PVN, nucleus reuniens, and medial tip of the zona incerta. In case 110 the FG injection site filled the anterior PVN (e.g., bregma − 1.0 and −1.4 mm) and hit the dorsal edge of the PVN at mid-PVN levels (e.g., bregma −1.8 mm). This case had minimal FG spread into the peri-PVN and nucleus reuniens. In case 112 the FG site involved almost the entirety of the PVN at anterior (e.g., bregma −1.3 mm) and mid-PVN levels (e.g., bregma −1.7 mm). There was little FG spread into the peri-PVN and medial preoptic area/ nucleus. The FG injection site in case 102 included much of the posterior PVN (bregma −2.1 mm) and hit the dorsal edge of the PVN at mid-PVN levels (e.g., bregma −1.8 mm), as well as small amounts into the peri-PVN, anterior hypothalamic nucleus posterior subdivision, and medial tip of the zona incerta. The FG injection site in case 104 included much of the posterior PVN (bregma −2.1 mm) and hit the dorsal edge of the PVN at mid-PVN levels (e.g., bregma −1.8 mm), with small amounts into the nucleus reuniens and the medial tip of the zona incerta. In case 109 the FG site involved the medial portion of the PVN at mid- (bregma −1.8 mm) and posterior- (bregma −2.1 mm) PVN levels with some FG spread into the contralateral medial PVN, the nucleus reuniens, and the medial tip of the zona incerta. An initial analysis indicated that in several forebrain regions the number of retrogradely labeled FG cells varied with the rostral-to-caudal extent of the FG injection site in the PVN. Therefore, subsequent analyses were conducted by dividing the cases into two groups: those that involved the anterior-to-mid PVN (cases 90, 110, and 112) and those that involved the mid-to-posterior PVN (cases 102, 104, and 109), with mid-PVN being defined as approximately bregma −1.8 mm, using the Paxinos and Watson coordinate system (1998).

Forebrain regions that contained substantial numbers of retrogradely labeled FG-positive cells (on average >10 from anterior and/or posterior PVN) are listed in Table 2, and include regions in the bed nucleus of the stria terminalis, hypothalamus, and thalamus. It should be noted that in addition to the cell counts presented on Table 2, a few FG-positive cells (on average <5 per region) were occasionally observed in the nucleus of the diagonal band and subregions of the amygdala (e.g., central and cortical), thalamus (e.g., reticular, and parataenial) and hypothalamus (e.g., anterodorsal preoptic nucleus, anteroventral preoptic nucleus, supraoptic nucleus, and the anterior part of the ventromedial nucleus; for abbreviations, see Table 3), but the low incidence in these regions precluded further quantification of VGluT colocalization. Low numbers of FG-positive cells were commonly observed in the subfornical area and organum vasculosum of the lamina terminalis and many of these appeared to be VGluT2-positive; however, the low prevalence precluded further quantification. Similarly, low numbers of FG-positive cells were occasionally observed in the anterior PVN following FG injections targeted to the posterior PVN but the low prevalence precluded quantification.

VGluT1 and VGluT2 mRNA expression

Robust expression of VGluT1 mRNA was observed in the cerebral cortex, hippocampus, medial habenula, and lateral amygdala, as previously noted (Ziegler et al., 2002). Weaker VGluT1 mRNA hybridization signal (diffuse labeling) was observed in hypothalamic nuclei, including the PVN and supraoptic nucleus. Only a few double-labeled FG/VGluT1-positive

neurons (Fig. 2) were observed in the forebrain, and the frequency of these neurons was too low to permit quantification.

VGluT2 mRNA was highly expressed in the habenula (medial and lateral), thalamus, and hypothalamus, including the ventromedial hypothalamic nucleus, anteroventral periventricular nucleus, preoptic nuclei, dorsomedial hypothalamic nucleus, posterior hypothalamic nucleus, lateral hypothalamic area, and mammillary nuclei, as noted previously (Ziegler et al., 2002). More moderate expression of VGluT2 mRNA was noted in portions of the medial amygdala, substantia innominata, bed nucleus of the stria terminalis, zona incerta, anterior hypothalamic nucleus, tuberal nucleus, and retrochiasmatic area, often limited to scattered cells. By comparison, the PVN and supraoptic nucleus expressed low levels of VGluT2 mRNA (diffuse labeling lacking cellular resolution). Numerous double-labeled FG/VGluT2-positive neurons (Fig. 2) were observed throughout forebrain, with some notable variations depending on the rostral-to-caudal extent of the FG injection site in the PVN. Therefore, subsequent results are presented divided into two groups: FG injection sites in anterior-to-mid PVN versus in mid-to-posterior PVN.

VGlut2-innervation to anterior PVN

Following FG injection in the anterior PVN and its surround (Table 2; Fig. 3), high numbers of FG-positive cell bodies were observed ipsilaterally in the anterior hypothalamic area and nucleus, lateral hypothalamic area, medial preoptic area and nucleus, ventromedial hypothalamic nucleus, medial amygdala, and zona incerta. Among these regions, only the ventromedial hypothalamic nucleus represented a primary source of VGluT2-positive innervation, with ≈25% of the FG-labeled cells colabeling for VGluT2.

More moderate numbers of FG-positive cell bodies were found ipsilaterally in the bed nucleus of the stria terminals (anterodorsal, anteroventral, interfascicular/ventral, and principle subdivisions), arcuate nucleus, dorsomedial hypothalamic nucleus, lateral preoptic area, median preoptic area, posterior hypothalamic nucleus, periventricular hypothalamic nucleus, retrochiasmatic area, suprachiasmatic nucleus, tuberal nucleus, paraventricular thalamic nucleus, lateral septum, and substantia innominata after injection in the anterior PVN and its surround. These regions generally contributed little-to-no VGluT2-positive innervation to the anterior PVN and its surround (less than 15% colocalization).

Contralateral to the FG injection site (data not shown), the pattern of FG-positive cell labeling was generally similar to that observed ipsilaterally; however, the total number of FG-positive cells in each region was substantially lower. Moreover, FG coexpression with VGluT2 was low throughout contralateral forebrain (less than 15%).

VGlut2-innervation to posterior PVN

FG injection into the posterior PVN and its surround (Table 2; Fig. 3) produced high numbers of FG-positive cell bodies in the anterior hypothalamic nucleus, lateral hypothalamic nucleus, posterior hypothalamic nucleus, ventromedial hypothalamic nucleus, lateral septum, and zona incerta. Of these regions, the ventromedial hypothalamic nucleus and posterior hypothalamic nucleus were major sources of VGluT2 innervation to the posterior PVN, with ≈80% and 60% colocalization, respectively. The anterior hypothalamic nucleus and lateral hypothalamic area also contributed VGluT2 innervation, with ≈25% colocalization. In contrast, the lateral septum and zona incerta contributed little-to-no VGluT2 innervation to the posterior PVN and its surround (less than 5% colocalization).

More moderate numbers of FG-positive cells were consistently located in the bed nucleus of the stria terminalis (anteroventral and interfascicular/ventral subdivisions), dorsomedial hypothalamic nucleus, lateral preoptic area, medial preoptic area and nucleus,

paraventricular thalamic nucleus, medial amygdala, and substantia innominata following FG injection into the posterior PVN and its surround. Among these regions a large proportion of the FG-positive cells coexpressed VGluT2 in the paraventricular thalamic nucleus (≈80%), medial amygdala (≈50%), and dorsomedial hypothalamic nucleus (≈40%). Significantly fewer FG-positive cells colabeled for VGluT2 in the bed nucleus of the stria terminalis, lateral preoptic area, medial preoptic area and nucleus, and substantia innominata (generally no more than 15% colocalization).

Contralateral to the FG injection site (data not shown), the pattern of FG-positive cell labeling was generally similar to that observed ipsilaterally; however, the total number of FG-positive cells in each region was reduced. Moreover, FG coexpression with VGluT2 was still high in the contralateral ventromedial hypothalamic nucleus (≈80%), paraventricular thalamic nucleus (80%), and posterior hypothalamus (≈70%); moderate in the anterior hypothalamic nucleus (25%), lateral hypothalamic area (25%), medial amygdala (35%), and dorsomedial hypothalamic nucleus (40%); and low in the bed nucleus of the stria terminalis, lateral preoptic area, medial preoptic area and nucleus, lateral septum, substantia innominata, and zona incerta (generally less than 15%).

Anterograde PhaL labeling from ventromedial nucleus to PVN

Three cases (11, 13, and 15) contained PhaL injection sites in the ventromedial nucleus. In case 11 the PhaL site involved the dorsomedial subdivision, central subdivision, and the dorsal portion of the ventrolateral subdivision, with only minimal spread dorsally into the dorsomedial hypothalamic nucleus. The PhaL injection site in case 13 included the lateral portions of the dorsomedial and central subdivision and the dorsal portion of the ventrolateral subdivision, with minimal lateral spread into the lateral hypothalamic area. The PhaL injection site in case 15 included the dorsomedial subdivision, the medial portion of the central subdivision, and the mediodorsal portion of the ventrolateral subdivision, with minimal spread beyond the ventromedial nucleus. The PhaL labeling produced in the PVN was similar for all three cases; representative images from cases 13 and 15 are shown in Figure 4. The anterior PVN contained numerous PhaL-positive fibers and boutons throughout the nucleus. The posterior PVN showed few PhaL-positive fibers and the mid-PVN contained an intermediate amount; at theses levels PhaL-positive fibers and boutons were present only in the medial (e.g., parvocellular) portions of the nucleus. Dual immunolabeling for PhaL and VGluT2 showed that while the posterior PVN contains a relatively small number of PhaL-positive boutons, most colabel with VGluT2 immunoreactivity (Fig. 4F,J,K,L). In contrast, the anterior PVN receives a richer innervation of PhaL-positive fibers and boutons, and while several colabel for VGluT2 there are also numerous PhaL fibers with boutons that do not colabel, suggesting other neurotransmitter phenotypes (Fig. 4E,G–I).

Anterograde PhaL labeling from posterior hypothalamic nucleus to PVN

Two cases (8 and 10) contained PhaL injection sites targeted to the posterior hypothalamic nucleus. The PhaL injection site in case 8 was located in the dorsal portion of the posterior nucleus with minimal spread beyond the nucleus. In case 10 the PhaL injection site was similarly located but with a bit of spread dorsal to the nucleus. The PhaL labeling produced in the PVN was similar for both cases; representative images from case 8 are shown in Figure 5. The anterior PVN (≈bregma −0.8 mm) contained few PhaL-positive fibers and boutons, whereas mid PVN (≈bregma −1.8 mm) contained several PhaL-positive fibers and boutons, particularly in the parvocellular subdivision. In the posterior PVN (≈bregma −2.1 mm) there were numerous PhaL-positive fibers and boutons throughout the PVN. Moreover, PhaL-positive fibers were most dense in the PVN surround at the mid and posterior levels.

Boutons dual-labeled for PhaL and VGluT2 were rarely observed in the anterior PVN, but commonly observed in the posterior PVN.

Anterograde PhaL labeling from medial preoptic hypothalamic nucleus to PVN

Two cases (18 and 20) contained PhaL injection sites targeted to the medial preoptic hypothalamic nucleus. The PhaL injection site in case 18 was located in the rostral portion of the medial preoptic nucleus, with minimal spread beyond the nucleus. In case 20 the PhaL injection site included the lateral subdivision, central subdivision, and lateral portion of the medial subdivision, with minimal spread into the lateral hypothalamic area. The PhaL labeling produced in the PVN was similar for both cases; representative images from case 20 are shown in Figure 6. The anterior PVN (≈bregma −0.8 mm) contained numerous PhaL-positive fibers and boutons, with even higher levels in the PVN surround. Mid and posterior PVN had few PhaL fibers in the medial portions of the nucleus, with even less in the lateral PVN. Notably, boutons dual labeled for PhaL and VGluT2 were not observed in the PVN regardless of rostral-caudal level.

DISCUSSION

Sources of forebrain glutamatergic innervation to the PVN and its surround were determined by combining retrograde FG labeling from the PVN with in situ hybridization for VGluT1 and VGluT2 mRNA. VGluT1 mRNA was highly expressed in cerebral cortex, hippocampus, habenula, and cortical amygdala, with considerably less expression in hypothalamic regions, as described previously (Kaneko and Fujiyama, 2002; Ziegler et al., 2002; Collin et al., 2003). Dual labeling with FG revealed only occasional double-labeled cells throughout the hypothalamus, with no double-labeling being observed in other forebrain sites. These data show that VGluT1-positive neurons do not constitute major sources of direct glutamatergic innervation to the PVN, as suggested by the presence of few VGluT1-positive nerve fibers in the PVN (Wittmann et al., 2005). These data also support the idea that forebrain regions containing VGluT1-positive neurons (e.g., hippocampus and cerebral cortex) provide information to the PVN via indirect circuits that utilize at least one intervening synapse (Herman et al., 2003). In contrast, VGluT2 mRNA was highly expressed in the habenula, as well as in numerous hypothalamic and thalamic nuclei, as described previously (Ziegler et al., 2002; Lin et al., 2003; Hur and Zaborszky, 2005; Barroso-Chinea et al., 2007). Dual labeling with FG showed many double-labeled neurons throughout the forebrain, particularly in the ventromedial hypothalamic nucleus, posterior hypothalamic nucleus, lateral hypothalamic area, anterior hypothalamic nucleus, dorsomedial hypothalamic nucleus, paraventricular thalamic nucleus, and medial amygdala. These data demonstrate that VGluT2-positive neurons contribute direct glutamatergic innervation to the PVN and its surround, and originate in hypothalamic, thalamic, and amygdalar brain regions. This work is consistent with earlier light and electron microscopy studies showing that the PVN contains numerous VGluT2-positive nerve fibers that contact corticotropin-releasing hormone and thyrotropin-releasing hormone neurons (Wittmann et al., 2005; Ziegler et al., 2005), and autoradiographic visualization of [^{3}H]D-aspartate transport identifies many of the same brain regions as potential sources of glutamatergic/aspartatergic innervation to the PVN (Csaki et al., 2000). Importantly, the proportion of FG labeled neurons that colabeled for VGluT2 mRNA varied with the rostral-to-caudal extent of the FG injection site within the PVN. When FG injections were targeted to the anterior PVN, colocalization with VGluT2 was most common in the ventromedial hypothalamic nucleus (≈25% of neurons). However, when FG injections were targeted to the posterior PVN, colocalization with VGluT2 was most common in the ventromedial hypothalamic nucleus (≈80% of neurons), paraventricular thalamic nucleus (≈80%), posterior hypothalamic nucleus (≈60%), medial amygdala (≈50%), dorsomedial hypothalamic

nucleus (≈40%), anterior hypothalamic nucleus (≈25%), and lateral hypothalamic area (≈25%). Moreover, anterograde PhaL tract tracing combined with VGluT2 immunolabeling showed that 1) ventromedial nucleus-derived glutamatergic inputs occur in both the anterior and posterior PVN; 2) posterior nucleus-derived glutamatergic inputs occur predominantly in the posterior PVN; and 3) medial preoptic nucleus-derived inputs to the PVN are not glutamatergic, thereby independently corroborating the innervation pattern. These data suggest that the extent of PVN innervation by VGluT2-positive neurons varies between the anterior and posterior portions of the nucleus and may have important implications for PVN regulation (discussed further below).

In the present work, FG labeling from the PVN and its surround identified numerous forebrain sites that contained PVN/surround-projecting neurons (Table 2). This pattern of retrograde labeling from the PVN mirrors that reported by others (Berk and Finkelstein, 1981; Tribollet and Dreifuss, 1981; Sawchenko and Swanson, 1983; Campeau and Watson, 2000), including the observation that retrograde labeling in the medial amygdala is greater after injections into the anterior PVN (Sawchenko and Swanson, 1983). In addition, the PVN/surround-projecting forebrain regions identified in the present study are consistent with anterograde labeling studies. For instance, the present data using PhaL tract tracing from the ventromedial, posterior, and medial preoptic hypothalamic nuclei, taken together with prior anterograde tract-tracing studies, demonstrate that the anterior hypothalamic area and nucleus, dorsomedial hypothalamic nucleus, lateral hypothalamic area, medial preoptic area and nucleus, posterior hypothalamic nucleus, ventromedial hypothalamic nucleus, paraventricular thalamic nucleus, medial amygdala, lateral septum, substantia innominata, and zona incerta project fibers into the PVN (Chiba and Murata, 1985; ter Horst and Luiten, 1986, 1987; Grove, 1988; Simerly and Swanson, 1988; Canteras et al., 1994; Risold et al., 1994; Canteras et al., 1995; Vertes et al., 1995; Wagner et al., 1995; Thompson et al., 1996; Risold and Swanson, 1997; Prewitt and Herman, 1998) and/or peri-PVN regions (Ter Horst and Luiten, 1987; Simerly and Swanson, 1988; Canteras et al., 1994, 1995; Risold et al., 1994; Moga et al., 1995; Vertes et al., 1995; Risold and Swanson, 1997). Of note, a more limited number of FG-positive neurons were observed in numerous other forebrain sites, including the subfornical area and organum vasculosum of the lamina terminalis, which are known to provide direct input to the PVN (Swanson and Lind, 1986; Larsen and Mikkelsen, 1995; Duan et al., 2008; Shi et al., 2008). In these particular regions the number of FG-positive cells was too low to permit quantification of VGluT2 colocalization, possibly because the relatively small size of these structures leads to infrequent sampling, thereby providing fewer opportunities to visualize the cells. However, we did observe several FG-positive cells in these regions that were also positive for VGluT2 mRNA, suggesting that at least some of the direct PVN projections from the subfornical organ and organum vasculosum of the lamina terminalis are glutamatergic (Antunes et al., 2006).

Moreover, the present study assessed potential differential weighting of forebrain inputs to the anterior versus posterior portions of the PVN. Following FG injections targeted to the anterior PVN, more FG neurons were seen in the anterior hypothalamic area and nucleus (central subdivision), arcuate nucleus, bed nucleus of the stria terminalis, medial amygdala, median preoptic area, medial preoptic area and nucleus, retrochiasmatic area, reticular thalamic nucleus, suprachiasmatic nucleus, tuberal nucleus, and ventromedial hypothalamic nucleus than with FG targeting to the posterior PVN, suggesting that these forebrain sites may provide relatively greater inputs to the anterior (versus posterior) PVN. Anterograde PhaL tract tracing from the ventromedial hypothalamic nucleus (Fig. 4), medial preoptic nucleus (Fig. 6), and ventral medial amygdala (data not shown) corroborates this idea, in that a higher density of PhaL fibers derived from these structures were observed in the anterior versus posterior PVN. In addition, others have shown that anterograde labeling from the central subdivision of the anterior hypothalamic nucleus (Risold et al., 1994),

anterodorsal preoptic nucleus (Thompson and Swanson, 2003), anteroventral preoptic nucleus (Thompson and Swanson, 2003), medial preoptic nucleus (Thompson and Swanson, 2003), retrochiasmatic area (Ribeiro-Barbosa et al., 1999), ventral medial amygdala (Prewitt and Herman, 1998), and ventromedial hypothalamic nucleus (Canteras et al., 1994) yields more fibers in the rostral versus caudal PVN, consistent with the retrograde labeling observed presently. In contrast, similar numbers of FG neurons were seen in the lateral hypothalamic area following anterior and posterior PVN injections, suggesting that the extent of lateral hypothalamic area input does not vary over the rostral-to-caudal extent of the nucleus. Following FG targeted to the posterior PVN, larger numbers of FG neurons were observed in the dorsomedial hypothalamic nucleus, lateral preoptic area, lateral septum, posterior hypothalamic nucleus, paraventricular thalamic nucleus, substantia innominata, and zona incerta relative to anterior PVN injections, suggesting that the posterior PVN and its surround may receive greater forebrain inputs from these regions. Anterograde PhaL tract tracing from the posterior hypothalamic nucleus (Fig. 5) revealed greater numbers of PhaL-positive fibers and boutons in the posterior (versus anterior) PVN, supporting this pattern of innervation. However, anterograde labeling from the lateral septum (data not shown) confirmed innervation primarily of the PVN surround, with little entering the PVN itself (Risold and Swanson, 1997), regardless of rostral-caudal level. FG-positive neurons in the lateral septum following injection targeted to the PVN probably resulted from the unavoidable spread of small amounts of FG into the immediate vicinity of the PVN. For example, the lateral septum projects to the reuniens nucleus of the thalamus, the zona incerta, and the peri-PVN (Risold and Swanson, 1997). The spread of FG likely occurred to a larger extent for the posterior PVN, where the shape of the nucleus becomes laterally elongated such that the circular-shaped FG injection inevitably spreads further beyond the dorsal and/or ventral boundaries of the nucleus. Notably, the collective innervation pattern of the PVN seems to generally follow a spatial map, with anterior and mid-level hypothalamic regions (anterior hypothalamic area/nucleus, arcuate, median preoptic, medial preoptic, retrochiasmatic, suprachiasmatic, tuberal, and ventromedial nuclei) being identified as providing innervation preferentially to anterior-mid PVN, and with mid-level and posterior hypothalamic regions (dorsomedial and posterior nuclei) being identified as providing innervation preferentially to mid-posterior PVN.

Anterograde labeling from the ventromedial, posterior, and medial preoptic hypothalamic nuclei was combined with VGluT2 immunolabeling to determine 1) whether any observed colabeling of FG and VGluT2 mRNA in these sites originated from the PVN itself versus its immediate surround; and 2) whether the density of PVN glutamatergic innervation from these sites varied across the rostral-to-caudal extent of the nucleus. Ventromedial nucleus-derived PhaL fibers and boutons were present throughout the PVN, with the highest density occurring in the anterior portion of the nucleus. Colabeling of these PhaL fibers with VGluT2 immunoreactivity often occurred in the PVN regardless of rostral-caudal level, suggesting that the ventromedial nucleus is a source of PVN glutamatergic innervation across the entire rostral-caudal extent of the nucleus. In contrast, posterior hypothalamic nucleus-derived PhaL fibers and boutons occurred with greatest frequency in the posterior PVN, as did colabeled boutons for VGluT2 immunoreactivity, suggesting that the posterior nucleus contributes glutamatergic innervation predominantly to the posterior PVN. Medial preoptic nucleus-derived PhaL fibers and boutons were most prevalent in the anterior PVN; however, colabeling with VGluT2 was not observed regardless of rostral-caudal level, suggesting that the medial preoptic nucleus uses other neurotransmitters (e.g., GABA) and does not contribute glutamatergic innervation to the PVN. Additional anterograde labeling studies will be needed to confirm differential glutamatergic innervation of the PVN by the other implicated forebrain regions. However, the collective work supports the contention that glutamatergic innervation of the anterior-to-mid PVN and its surround is largely derived from the ventromedial hypothalamic nucleus, whereas glutamatergic innervation of the mid-

to-posterior PVN and its surround originates primarily in the ventromedial, lateral, posterior, and dorsomedial hypothalamic nuclei.

Methodological considerations

The irregular geometries of the anterior and posterior PVN present a significant barrier to retrograde tract-tracing studies. In the current report we endeavored to interpret our data with respect to both the present and previous anterograde tracing studies. Nonetheless, we need to acknowledge that VGlut2 innervation of the PVN proper (versus the PVN-surround) may be overestimated by the retrograde labeling approach.

Immunohistochemical analyses of VGluT1 and VGluT2 immunoreactivity indicate nearly exclusive localization in terminals (Herzog et al., 2001; Lin et al., 2003). This staining pattern prohibits use of dual immunohistochemistry for colocalization of VGluT1 or VGluT2 immunoreactivity in FG-positive neuronal cell bodies. The double-labeling approach used here provides a reliable and proven colocalization method for immunoreactivity and mRNA. However, visualization of colocalization requires imaging silver grains in a thin emulsion layer atop a 30 μm section (see Fig. 2 for example). We have taken a conservative approach to identifying FG-positive neurons and confirming mRNA colocalization, and may be missing colocalization in FG-positive cells that are relatively deep within the tissue section or whose morphology did not clearly resemble a cell body. In addition, the fact that radioactive grains lie in an emulsion layer above cellular sources probably causes us to miss radioactive sources lying deep in the section. Thus, the current report likely under-estimates the number of VGluT2/FG colocalized cells. Alternatively, it is possible that VGluT mRNA expression is not a universal marker for glutamatergic neurons. Previous studies establish VGluT1 and VGluT2 mRNA as specific markers of the glutamatergic neurons (reviewed in Ziegler et al., 2002; Takamori, 2006), but it is not yet known if they are expressed in all glutamate neurons. Since our approach was consistent across animals, the overall proportion of colocalized cells in a given region can be compared between animals and injection sites.

Anterograde tract tracing with PhaL is a well-established approach that labels the efferent projections from injection sites. PhaL injection sites are relatively small, providing increased anatomical specificity at the expense of labeling the full extent of projecting neurons. Thus, the abundance of PhaL-positive labeling in the PVN following injection in the ventromedial, posterior, and medial preoptic hypothalamic nuclei reflects labeling of only a subset of neurons in these areas. Importantly, PhaL labels both the projecting fibers and their terminals/boutons, providing the ability to coimmunolabel for VGluT2 (which localizes only to glutamatergic nerve terminals). In this manner, the proportion of PhaL-positive terminals that colabel with VGluT2 can be visualized. However, since PhaL also labels projecting fibers (versus VGluT2 immunoreactivity, which is only detected in terminals), quantifying the relative amount of PhaL labeling that is dual-labeled for VGluT2 cannot provide a meaningful representation of the amount of PhaL-positive terminals that are colabeled. Hence, the most appropriate manner to view this material is to gauge the relative proportion of PhaL-positive terminals (excluding the fibers) that are colabeled for VGluT2.

We should note that we have not included VGluT3 in our analyses, as the present literature does not support it as a major source of forebrain glutamatergic input to the PVN (Gras et al., 2002; Schafer et al., 2002; Herzog et al., 2004). VGluT3 mRNA is present in rodent brain at levels much below that of VGluT1 and VGluT2, and with a much more limited forebrain distribution (e.g., scattered cells of striatum, hippocampus, and neocortex) (Gras et al., 2002; Schafer et al., 2002; Herzog et al., 2004). Moreover, VGluT3 mRNA expression appears to largely occur in interneurons and/or brain regions that are known to have little-to-no direct projections to the PVN (Gras et al., 2002; Schafer et al., 2002; Herzog et al., 2004),

thus the present work focuses on VGluT1 and VGluT2 as the primary potential sources of forebrain glutamatergic input to the PVN.

Functional considerations

An important consideration of the present work is the relative abundance (and hence functional importance) of glutamatergic innervation to the PVN. Clearly some sources of innervation (e.g., posterior hypothalamic nucleus, Fig. 5) provide a denser innervation to the PVN-surround than to the PVN itself. The PVN surround contains neurons that project into the PVN and regulate its function (Herman et al., 2002), thereby providing an indirect means for PVN regulation by the posterior hypothalamic nucleus. Additionally, the posterior hypothalamic nucleus provides a more modest direct innervation to the PVN itself, particularly to the middle and posterior portions. Given the preponderance of multiple types of glutamate receptors throughout the PVN, including the presence of NMDA-type receptors that function to dramatically amplify glutamatergic signaling (Herman et al., 2000), even a relatively modest number of glutamatergic inputs could contribute significantly to neuronal signaling and PVN function. Moreover, the methods employed invariably underestimate the full extent of glutamatergic inputs (see Methodological considerations, above), suggesting that the most appropriate interpretations are not from the actual percentage of colabeling reported, but rather from comparing the relative abundance among the various injection sites (e.g., anterior versus posterior FG injection sites). Finally, the PVN proper has a considerable neuronal density, whereas the surround is rich in fibers. Thus, the relative amount of fiber input into the PVN proper will likely appear lower than the surround, due to the space occupied by the relatively large neuronal somata and their dendrites.

The observed rostral-to-caudal variations in the innervation of the PVN and its surround may have important functional implications. The PVN is comprised of connectionally distinct subregions, which vary in position and orientation over the rostral-caudal extent of the nucleus (reviewed in Sawchenko and Swanson, 1983). For example, the anterior-to-middle portion of the PVN is enriched in thyrotropin-releasing hormone neurons (e.g., anterior, medial, and periventricular parvocellular divisions; Lechan and Segerson, 1989), whereas the middle-to-posterior PVN contains relatively larger amounts of preautonomic neurons (Sawchenko and Swanson, 1983). Moreover, the anterior magnocellular PVN primarily contains oxytocinergic neurons, whereas the posterior PVN contains both oxytocinergic and vasopressinergic magnocellular neurons (Sawchenko and Swanson, 1983). Based on this, one might predict that PVN functions mediated by glutamatergic regulation of the anterior PVN are influenced largely by the ventromedial hypothalamic nucleus, whereas functions mediated by glutamatergic regulation of the posterior PVN are predominantly influenced by the ventromedial hypothalamic nucleus, lateral hypothalamic area, posterior hypothalamic nucleus, and dorsomedial hypothalamic nucleus.

In general, the anterior PVN region is lacking a significant VGluT2 innervation from forebrain structures, with the exception of the ventromedial hypothalamus. Regions projecting into the anterior PVN are generally rich in GABAergic and peptidergic neurons (cf. Harlan et al., 1987; Simerly and Swanson, 1987; Okamura et al., 1990), suggesting that forebrain regulation of this region may be accomplished primarily by these nonglutamatergic neuronal inputs. The fact that the ventromedial nucleus is the primary source of forebrain glutamate anterior PVN input is intriguing, given its role in satiety mechanisms and glucose regulation (King, 2006). The anterior-to-mid PVN is enriched in neuroendocrine TRH cells that are implicated in metabolic regulation (Lechan and Fekete, 2006), suggesting the potential for glutamate-mediated activation of thyroid hormone release. It is also important to consider that the anterior PVN contains non-neuroendocrine neurons that innervate the lateral septum as well as brainstem sites (Swanson and Kuypers, 1980; Risold and Swanson, 1997), providing an opportunity for metabolic information to be

communicated to limbic regulators of body temperature and brainstem mediators of energy regulation.

The posterior PVN has by far the largest population of preautonomic (i.e., brainstem and spinal cord) projecting neurons in the nucleus (Sawchenko and Swanson, 1983). The more extensive network of posterior PVN region-projecting VGlut2 neuron suggests a prominent role of forebrain (particularly hypothalamic) glutamate in autonomic functions of the PVN, which include regulation of heart rate, blood pressure, and sympathetic nerve discharge (Badoer et al., 2003; Kenney et al., 2003; Li et al., 2006; Freeman and Brooks, 2007). The present data suggest a greater capacity for direct excitation of this region by glutamate, consistent with rapid relay of homeostatic input to autonomic effector systems.

The distribution of CRH neurons in the PVN straddles the anterior and posterior divisions (Swanson et al., 1987). These data suggest that the forebrain sources of input to CRH neurons may vary across along the rostrocaudal extent of the nucleus, with the anterior cell groups receiving VGluT2 innervation largely limited to the ventromedial hypothalamus, and the posterior regions receiving significant input from a number of forebrain sources. Possible rostrocaudal differences in input to CRH cell groups may reflect the composite role of CRH in energy balance and stress regulation.

Overall, the anterior–posterior differences in innervation patterns suggest that the relative role of forebrain glutamate projections is differentially distributed with respect to endogenous PVN cell populations. The data suggest a selective role for forebrain glutamate in control of PVN output and, thereby, homeostatic integration.

Acknowledgments

The authors thank C. Mark Dolgas for assistance with some of the tract-tracing surgeries.

Grant sponsor: National Institutes of Health (NIH); Grant numbers: MH049698 (to J.P.H.), MH069725 (to J.P.H.), DK059803 (to Y.M.U.), DK067820 (to Y.M.U.), and DK078906 (to Y.M.U.).

LITERATURE CITED

Antunes VR, Yao ST, Pickering AE, Murphy D, Paton JF. A spinal vasopressinergic mechanism mediates hyperosmolality-induced sympathoexcitation. J Physiol. 2006; 576(Pt 2):569–583. [PubMed: 16873404]

Aubry JM, Bartanusz V, Pagliusi S, Schulz P, Kiss JZ. Expression of ionotropic glutamate receptor subunit mRNAs by paraventricular corticotropin-releasing factor (CRF) neurons. Neurosci Lett. 1996; 205:95–98. [PubMed: 8907325]

Badoer E, Ng CW, De Matteo R. Glutamatergic input in the PVN is important in renal nerve response to elevations in osmolality. Am J Physiol Renal Physiol. 2003; 285:F640–F650. [PubMed: 12954592]

Barroso-Chinea P, Castle M, Aymerich MS, Perez-Manso M, Erro E, Tunon T, Lanciego JL. Expression of the mRNAs encoding for the vesicular glutamate transporters 1 and 2 in the rat thalamus. J Comp Neurol. 2007; 501:703–715. [PubMed: 17299752]

Berk ML, Finkelstein JA. Afferent projections to the preoptic area and hypothalamic regions in the rat brain. Neuroscience. 1981; 6:1601–1624. [PubMed: 7266881]

Bisset GW, Chowdrey HS. Control of release of vasopressin by neuroendocrine reflexes. Q J Exp Physiol. 1988; 73:811–872. [PubMed: 2907166]

Campeau S, Watson SJ Jr. Connections of some auditory-responsive posterior thalamic nuclei putatively involved in activation of the hypothalamo-pituitary-adrenocortical axis in response to audiogenic stress in rats: an anterograde and retrograde tract tracing study combined with Fos expression. J Comp Neurol. 2000; 423:474–491. [PubMed: 10870087]

Canteras NS, Simerly RB, Swanson LW. Organization of projections from the ventromedial nucleus of the hypothalamus: a Phaseolus vulgaris-leucoagglutinin study in the rat. J Comp Neurol. 1994; 348:41–79. [PubMed: 7814684]

Canteras NS, Simerly RB, Swanson LW. Organization of projections from the medial nucleus of the amygdala: a PHAL study in the rat. J Comp Neurol. 1995; 360:213–245. [PubMed: 8522644]

Chiba T, Murata Y. Afferent and efferent connections of the medial preoptic area in the rat: a WGA-HRP study. Brain Res Bull. 1985; 14:261–272. [PubMed: 3995367]

Collin M, Backberg M, Ovesjo ML, Fisone G, Edwards RH, Fujiyama F, Meister B. Plasma membrane and vesicular glutamate transporter mRNAs/proteins in hypothalamic neurons that regulate body weight. Eur J Neurosci. 2003; 18:1265–1278. [PubMed: 12956725]

Csaki A, Kocsis K, Halasz B, Kiss J. Localization of glutamatergic/aspartatergic neurons projecting to the hypothalamic paraventricular nucleus studied by retrograde transport of [3H]D-aspartate autoradiography. Neuroscience. 2000; 101:637–655. [PubMed: 11113313]

Duan PG, Kawano H, Masuko S. Collateral projections from the subfornical organ to the median preoptic nucleus and paraventricular hypothalamic nucleus in the rat. Brain Res. 2008; 1198:68–72. [PubMed: 18262505]

Eyigor O, Minbay Z, Cavusoglu I, Jennes L. Localization of kainate receptor subunit GluR5-immunoreactive cells in the rat hypothalamus. Brain Res Mol Brain Res. 2005; 136:38–44. [PubMed: 15893585]

Fehm HL, Kern W, Peters A. The selfish brain: competition for energy resources. Prog Brain Res. 2006; 153:129–140. [PubMed: 16876572]

Flak JN, Ostrander MM, Tasker JG, Herman JP. Chronic stress-induced neurotransmitter plasticity in the PVN. J Comp Neurol. 2009; 517:156–165. [PubMed: 19731312]

Freeman KL, Brooks VL. AT(1) and glutamatergic receptors in paraventricular nucleus support blood pressure during water deprivation. Am J Physiol Regul Integr Comp Physiol. 2007; 292:R1675–R1682. [PubMed: 17185407]

Gras C, Herzog E, Bellenchi GC, Bernard V, Ravassard P, Pohl M, Gasnier B, Giros B, El Mestikawy S. A third vesicular glutamate transporter expressed by cholinergic and serotoninergic neurons. J Neurosci. 2002; 22:5442–5451. [PubMed: 12097496]

Graziano A, Liu XB, Murray KD, Jones EG. Vesicular glutamate transporters define two sets of glutamatergic afferents to the somatosensory thalamus and two thalamocortical projections in the mouse. J Comp Neurol. 2008; 507:1258–1276. [PubMed: 18181146]

Grove EA. Efferent connections of the substantia innominata in the rat. J Comp Neurol. 1988; 277:347–364. [PubMed: 2461973]

Harlan RE, Shivers BD, Romano GJ, Howells RD, Pfaff DW. Localization of preproenkephalin mRNA in the rat brain and spinal cord by in situ hybridization. J Comp Neurol. 1987; 258:159–184. [PubMed: 3584538]

Herman JP, Eyigor O, Ziegler DR, Jennes L. Expression of ionotropic glutamate receptor subunit mRNAs in the hypothalamic paraventricular nucleus of the rat. J Comp Neurol. 2000; 422:352–362. [PubMed: 10861512]

Herman JP, Tasker JG, Ziegler DR, Cullinan WE. Local circuit regulation of paraventricular nucleus stress integration: glutamate-GABA connections. Pharmacol Biochem Behav. 2002; 71:457–468. [PubMed: 11830180]

Herman JP, Figueiredo H, Mueller NK, Ulrich-Lai Y, Ostrander MM, Choi DC, Cullinan WE. Central mechanisms of stress integration: hierarchical circuitry controlling hypothalamo-pituitary-adrenocortical responsiveness. Front Neuroendocrinol. 2003; 24:151–180. [PubMed: 14596810]

Herzog E, Bellenchi GC, Gras C, Bernard V, Ravassard P, Bedet C, Gasnier B, Giros B, El Mestikawy S. The existence of a second vesicular glutamate transporter specifies subpopulations of glutamatergic neurons. J Neurosci. 2001; 21:RC181. [PubMed: 11698619]

Herzog E, Gilchrist J, Gras C, Muzerelle A, Ravassard P, Giros B, Gaspar P, El Mestikawy S. Localization of VGLUT3, the vesicular glutamate transporter type 3, in the rat brain. Neuroscience. 2004; 123:983–1002. [PubMed: 14751290]

Hettes SR, Gonzaga J, Heyming TW, Perez S, Wolfsohn S, Stanley BG. Dual roles in feeding for AMPA/kainate receptors: receptor activation or inactivation within distinct hypothalamic regions elicits feeding behavior. Brain Res. 2003; 992:167–178. [PubMed: 14625056]

Hur EE, Zaborszky L. Vglut2 afferents to the medial prefrontal and primary somatosensory cortices: a combined retrograde tracing in situ hybridization study [corrected]. J Comp Neurol. 2005; 483:351–373. [PubMed: 15682395]

Kaneko T, Fujiyama F. Complementary distribution of vesicular glutamate transporters in the central nervous system. Neurosci Res. 2002; 42:243–250. [PubMed: 11985876]

Kenney MJ, Weiss ML, Haywood JR. The paraventricular nucleus: an important component of the central neurocircuitry regulating sympathetic nerve outflow. Acta Physiol Scand. 2003; 177:7–15. [PubMed: 12492774]

King BM. The rise, fall, and resurrection of the ventromedial hypothalamus in the regulation of feeding behavior and body weight. Physiol Behav. 2006; 87:221–244. [PubMed: 16412483]

Larsen PJ, Mikkelsen JD. Functional identification of central afferent projections conveying information of acute “stress” to the hypothalamic paraventricular nucleus. J Neurosci. 1995; 15:2609–2627. [PubMed: 7536817]

Lechan RM, Fekete C. The TRH neuron: a hypothalamic integrator of energy metabolism. Prog Brain Res. 2006; 153:209–235. [PubMed: 16876577]

Lechan RM, Segerson TP. Pro-TRH gene expression and precursor peptides in rat brain. Observations by hybridization analysis and immunocytochemistry. Ann N Y Acad Sci. 1989; 553:29–59. [PubMed: 2497675]

Li YF, Jackson KL, Stern JE, Rabeler B, Patel KP. Interaction between glutamate and GABA systems in the integration of sympathetic outflow by the paraventricular nucleus of the hypothalamus. Am J Physiol Heart Circ Physiol. 2006; 291:H2847–H2856. [PubMed: 16877560]

Lin W, McKinney K, Liu L, Lakhlani S, Jennes L. Distribution of vesicular glutamate transporter-2 messenger ribonucleic Acid and protein in the septum-hypothalamus of the rat. Endocrinology. 2003; 144:662–670. [PubMed: 12538629]

Mateos JM, Azkue J, Benitez R, Sarria R, Losada J, Conquet F, Ferraguti F, Kuhn R, Knopfel T, Grandes P. Immunocytochemical localization of the mGluR1b metabotropic glutamate receptor in the rat hypothalamus. J Comp Neurol. 1998; 390:225–233. [PubMed: 9453666]

McKenna KE. Neural circuitry involved in sexual function. J Spinal Cord Med. 2001; 24:148–154. [PubMed: 11585233]

Melis MR, Succu S, Mascia MS, Cortis L, Argiolas A. Extracellular excitatory amino acids increase in the paraventricular nucleus of male rats during sexual activity: main role of N-methyl-d-aspartic acid receptors in erectile function. Eur J Neurosci. 2004; 19:2569–2575. [PubMed: 15128410]

Moga MM, Weis RP, Moore RY. Efferent projections of the paraventricular thalamic nucleus in the rat. J Comp Neurol. 1995; 359:221–238. [PubMed: 7499526]

Nagy GM, Bodnar I, Banky Z, Halasz B. Control of prolactin secretion by excitatory amino acids. Endocrine. 2005; 28:303–308. [PubMed: 16388120]

Okamura H, Abitbol M, Julien JF, Dumas S, Berod A, Geffard M, Kitahama K, Bobillier P, Mallet J, Wiklund L. Neurons containing messenger RNA encoding glutamate decarboxylase in rat hypothalamus demonstrated by in situ hybridization, with special emphasis on cell groups in medial preoptic area, anterior hypothalamic area and dorsomedial hypothalamic nucleus. Neuroscience. 1990; 39:675–699. [PubMed: 2097521]

Paxinos, G.; Watson, C. The rat brain in stereotaxic coordinates. New York: Academic Press; 1998.

Prewitt CM, Herman JP. Anatomical interactions between the central amygdaloid nucleus and the hypothalamic paraventricular nucleus of the rat: a dual tracttracing analysis. J Chem Neuroanat. 1998; 15:173–185. [PubMed: 9797074]

Ribeiro-Barbosa ER, Skorupa AL, Cipolla-Neto J, Canteras NS. Projections of the basal retrochiasmatic area: a neural site involved in the photic control of pineal metabolism. Brain Res. 1999; 839:35–40. [PubMed: 10482796]

Risold PY, Swanson LW. Connections of the rat lateral septal complex. Brain Res Brain Res Rev. 1997; 24:115–195. [PubMed: 9385454]

Risold PY, Canteras NS, Swanson LW. Organization of projections from the anterior hypothalamic nucleus: a Phaseolus vulgaris-leucoagglutinin study in the rat. J Comp Neurol. 1994; 348:1–40. [PubMed: 7814679]

Sawchenko PE, Swanson LW. The organization of forebrain afferents to the paraventricular and supraoptic nuclei of the rat. J Comp Neurol. 1983; 218:121–144. [PubMed: 6886068]

Schafer MK, Varoqui H, Defamie N, Weihe E, Erickson JD. Molecular cloning and functional identification of mouse vesicular glutamate transporter 3 and its expression in subsets of novel excitatory neurons. J Biol Chem. 2002; 277:50734–50748. [PubMed: 12384506]

Schlenker EH. Integration in the PVN: another piece of the puzzle. Am J Physiol Regul Integr Comp Physiol. 2005; 289:R653–R655. [PubMed: 16105820]

Shi P, Martinez MA, Calderon AS, Chen Q, Cunningham JT, Toney GM. Intra-carotid hyperosmotic stimulation increases Fos staining in forebrain organum vasculosum laminae terminalis neurones that project to the hypothalamic paraventricular nucleus. J Physiol. 2008; 586(Pt 21):5231–5245. [PubMed: 18755745]

Simerly RB, Swanson LW. The distribution of neurotransmitter-specific cells and fibers in the anteroventral periventricular nucleus: implications for the control of gonadotropin secretion in the rat. Brain Res. 1987; 400:11–34. [PubMed: 2880634]

Simerly RB, Swanson LW. Projections of the medial preoptic nucleus: a Phaseolus vulgaris leucoagglutinin anterograde tract-tracing study in the rat. J Comp Neurol. 1988; 270:209–242. [PubMed: 3259955]

Swanson, LW. Brain maps: structure of the rat brain. Amsterdam: Elsevier; 1998.

Swanson LW, Kuypers HG. The paraventricular nucleus of the hypothalamus: cytoarchitectonic subdivisions and organization of projections to the pituitary, dorsal vagal complex, and spinal cord as demonstrated by retrograde fluorescence double-labeling methods. J Comp Neurol. 1980; 194:555–570. [PubMed: 7451682]

Swanson LW, Lind RW. Neural projections subserving the initiation of a specific motivated behavior in the rat: new projections from the subfornical organ. Brain Res. 1986; 379:399–403. [PubMed: 3742231]

Swanson LW, Sawchenko PE, Lind RW, Rho JH. The CRH motoneuron: differential peptide regulation in neurons with possible synaptic, paracrine, and endocrine outputs. Ann N Y Acad Sci. 1987; 512:12–23. [PubMed: 3327422]

Takamori S. VGLUTs: ‘exciting’ times for glutamatergic research? Neurosci Res. 2006; 55:343–351. [PubMed: 16765470]

ter Horst GJ, Luiten PG. The projections of the dorsomedial hypothalamic nucleus in the rat. Brain Res Bull. 1986; 16:231–248. [PubMed: 3697791]

ter Horst GJ, Luiten PG. Phaseolus vulgaris leuco-agglutinin tracing of intrahypothalamic connections of the lateral, ventromedial, dorsomedial and paraventricular hypothalamic nuclei in the rat. Brain Res Bull. 1987; 18:191–203. [PubMed: 2436726]

Thompson RH, Swanson LW. Structural characterization of a hypothalamic visceromotor pattern generator network. Brain Res Brain Res Rev. 2003; 41:153–202. [PubMed: 12663080]

Thompson RH, Canteras NS, Swanson LW. Organization of projections from the dorsomedial nucleus of the hypothalamus: a PHA-L study in the rat. J Comp Neurol. 1996; 376:143–173. [PubMed: 8946289]

Tribollet E, Dreifuss JJ. Localization of neurones projecting to the hypothalamic paraventricular nucleus area of the rat: a horseradish peroxidase study. Neuroscience. 1981; 6:1315–1328. [PubMed: 6167899]

van den Pol AN. Glutamate and aspartate immunoreactivity in hypothalamic presynaptic axons. J Neurosci. 1991; 11:2087–2101. [PubMed: 1676727]

Vertes RP, Crane AM, Colom LV, Bland BH. Ascending projections of the posterior nucleus of the hypothalamus: PHA-L analysis in the rat. J Comp Neurol. 1995; 359:90–116. [PubMed: 8557849]

Wagner CK, Eaton MJ, Moore KE, Lookingland KJ. Efferent projections from the region of the medial zona incerta containing A13 dopaminergic neurons: a PHA-L anterograde tract-tracing study in the rat. Brain Res. 1995; 677:229–237. [PubMed: 7552247]

Wittmann G, Lechan RM, Liposits Z, Fekete C. Glutamatergic innervation of corticotropin-releasing hormone- and thyrotropin-releasing hormone-synthesizing neurons in the hypothalamic paraventricular nucleus of the rat. Brain Res. 2005; 1039:53–62. [PubMed: 15781046]

Zhou J, Nannapaneni N, Shore S. Vessicular glutamate transporters 1 and 2 are differentially associated with auditory nerve and spinal trigeminal inputs to the cochlear nucleus. J Comp Neurol. 2007; 500:777–787. [PubMed: 17154258]

Ziegler DR, Herman JP. Local integration of glutamate signaling in the hypothalamic paraventricular region: regulation of glucocorticoid stress responses. Endocrinology. 2000; 141:4801–4804. [PubMed: 11108297]

Ziegler DR, Cullinan WE, Herman JP. Distribution of vesicular glutamate transporter mRNA in rat hypothalamus. J Comp Neurol. 2002; 448:217–229. [PubMed: 12115705]

Ziegler DR, Cullinan WE, Herman JP. Organization and regulation of paraventricular nucleus glutamate signaling systems: N-methyl-D-aspartate receptors. J Comp Neurol. 2005; 484:43–56. [PubMed: 15717303]

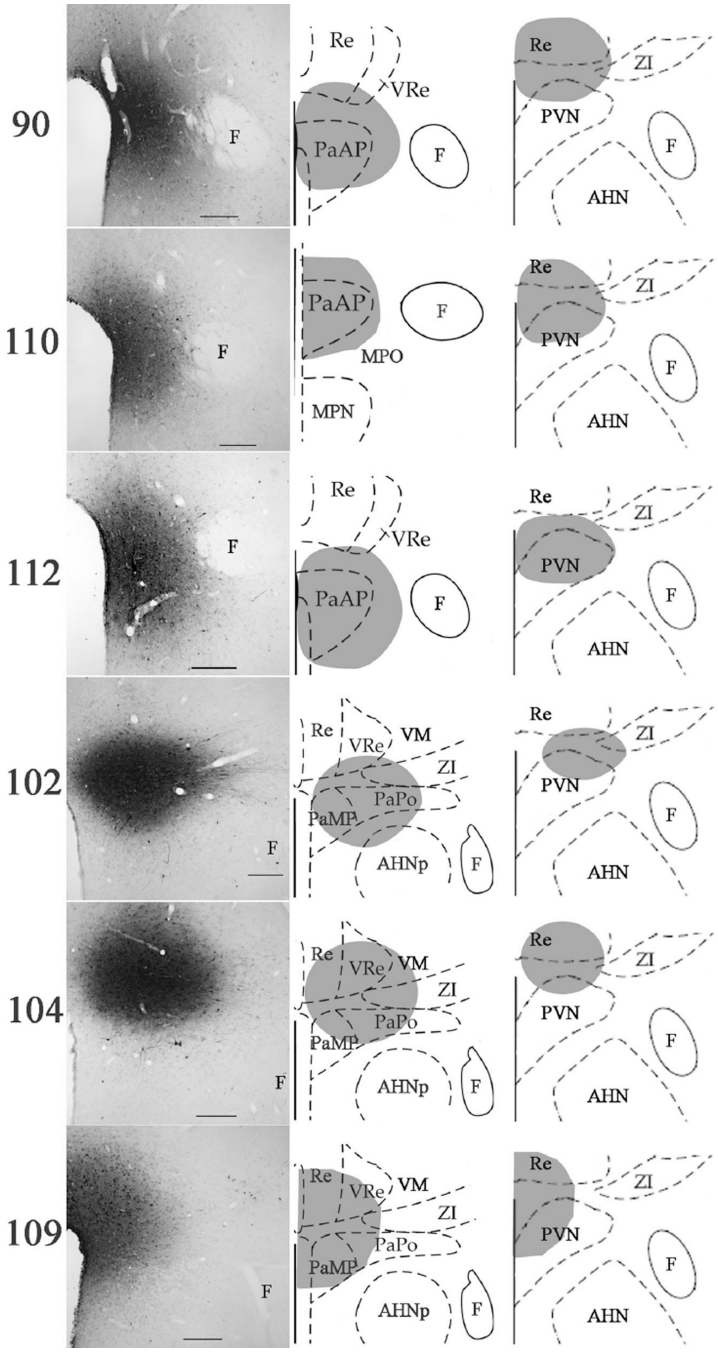

Figure 1.

FG-injection sites into the PVN and its surround showed varying involvement along the rostral-to-caudal extent of the nucleus. The anterior-to-mid portions of the PVN were primarily involved in cases 90 (≈bregma −1.4 mm for left and middle; ≈bregma −1.8 mm for right), 110 (≈bregma −1.3 mm for left and middle; ≈bregma −1.8 mm for right), and 112 (≈bregma −1.4 mm for left and middle; ≈bregma −1.8 mm for right), whereas the mid-to-posterior portions of the PVN were primarily involved in cases 102 (≈bregma −2.12 mm for left and middle; ≈bregma −1.8 mm for right), 104 (≈bregma −2.12 mm for left and middle; ≈bregma −1.8 mm for right), and 109 (≈bregma −2.12 mm for left and middle; ≈bregma −1.8 mm for right). Injection sites were imaged using brightfield microscopy (left)

and were mapped onto schematics (middle and right) modified from the Paxinos and Watson atlas (1998), following immunolabeling for FG with DAB visualization. Scale bars = 200 μm.

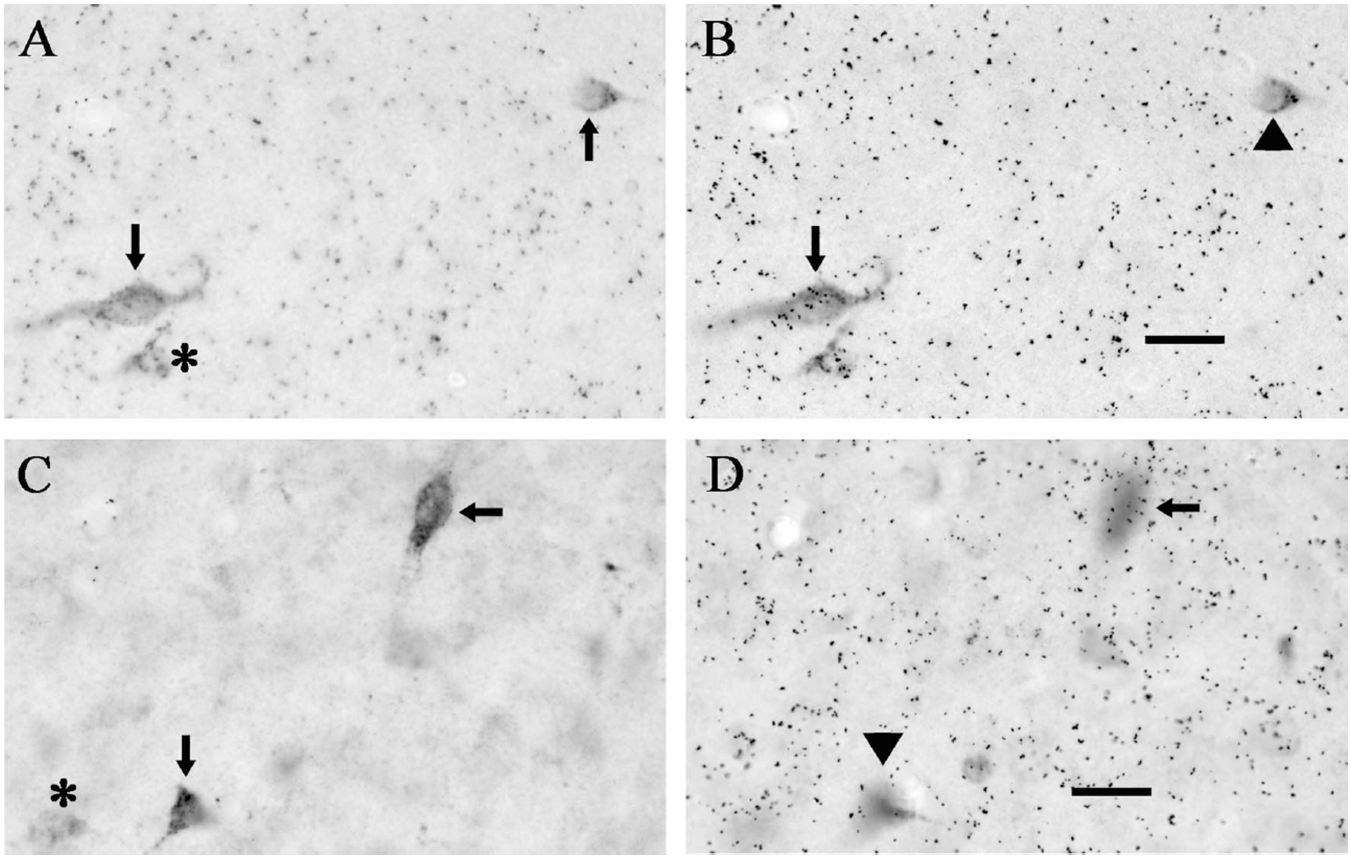

Figure 2.

Representative examples of cellular labeling for FG and vescicular glutamate transporter mRNA. **A**: Two FG-positive cells in the medial preoptic area; no other DAB labeling in the image reached criterion for quantification as an FG-positive neuron (asterisk). **B**: Focusing on the silver grains (black dots) that overlie the cells in panel A shows that one FG-positive cell is also positive for VGluT1 mRNA (arrow), whereas the other is not (arrowhead). Cells that colabeled for FG and VGluT1 mRNA were rarely observed in any of the examined brain regions. **C**: Two FG-positive cells in the ventromedial hypothalamic nucleus; no other DAB labeling in the image reached criterion for quantification as an FG-positive neuron (asterisk). **D**: Focusing on the silver grains (black dots) that overlie the cells in panel C shows that one FG-positive cell is also positive for VGluT2 mRNA (arrow), whereas the other is not (arrowhead). Also note that the background leve of hybridization was higher for VGluT1, so more silver grains (5× background) were required for a cell to be considered VGluT1-positive. Scale bars = 20 μm.

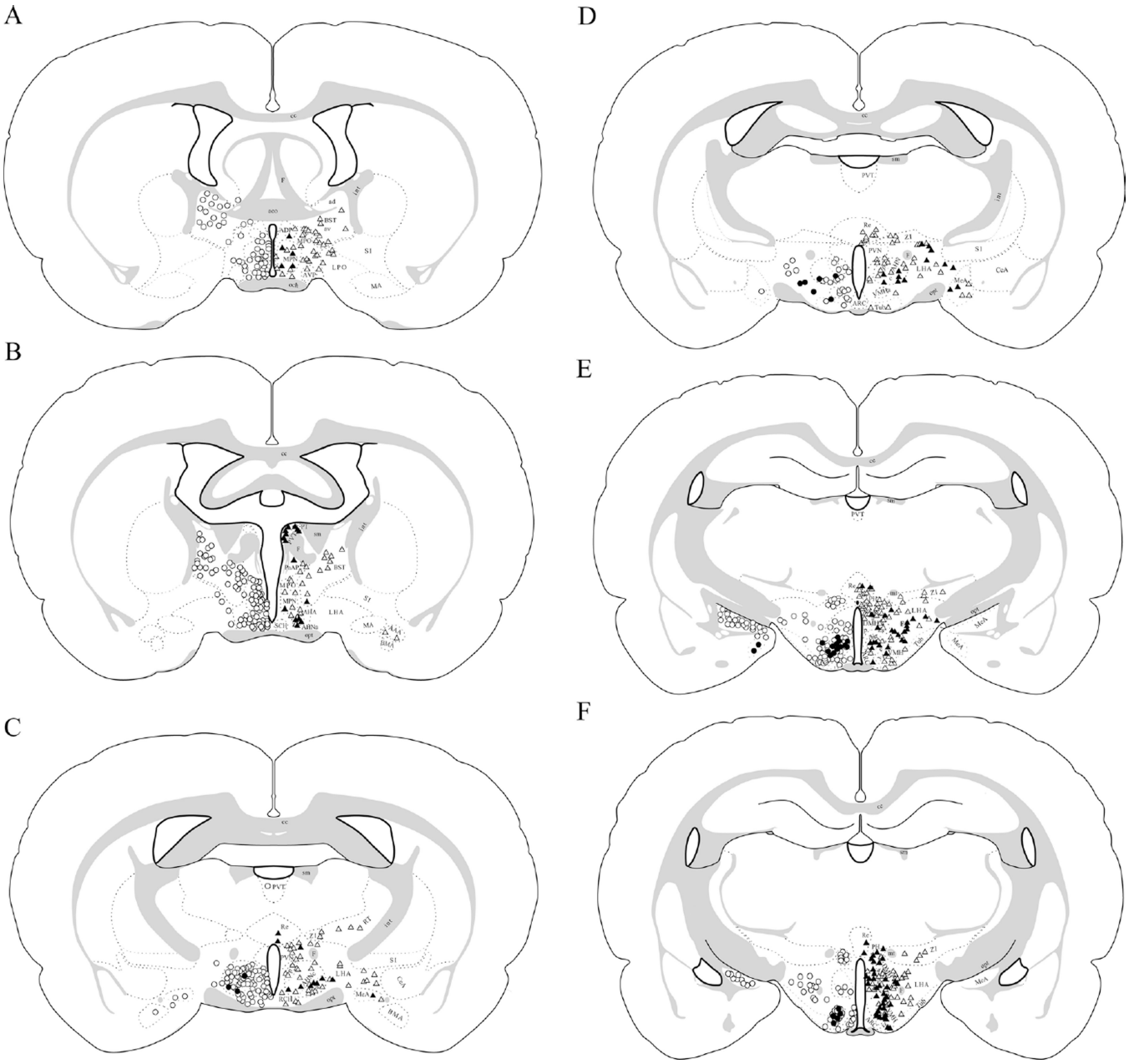

Figure 3.

FG injections into the anterior versus posterior PVN and its surround reveal differing extents of VGluT2 mRNA colocalization in PVN-projecting brain regions. Case 110 (anterior-to-mid PVN injection) is shown on the left side of the brain illustrations (open circles denote cells that are positive for FG only, whereas filled circles denote cells that are dual positive for FG and VGluT2 mRNA). Case 102 (posterior-to-mid PVN injection) is shown on the right side of the brain illustrations (open triangles denote cells that are positive for FG only, whereas filled triangles denote cells that are dual positive for FG and VGluT2 mRNA). **A**: ≈Bregma −0.4 mm. **B**: ≈Bregma −0.5 mm. **C**: ≈Bregma −1.55 mm. **D**: ≈Bregma −1.8 mm. **E**: ≈Bregma −2.8 mm. **F**: ≈Bregma −3.3 mm. Approximate cell locations were mapped onto schematics modified from the Swanson atlas (1998).

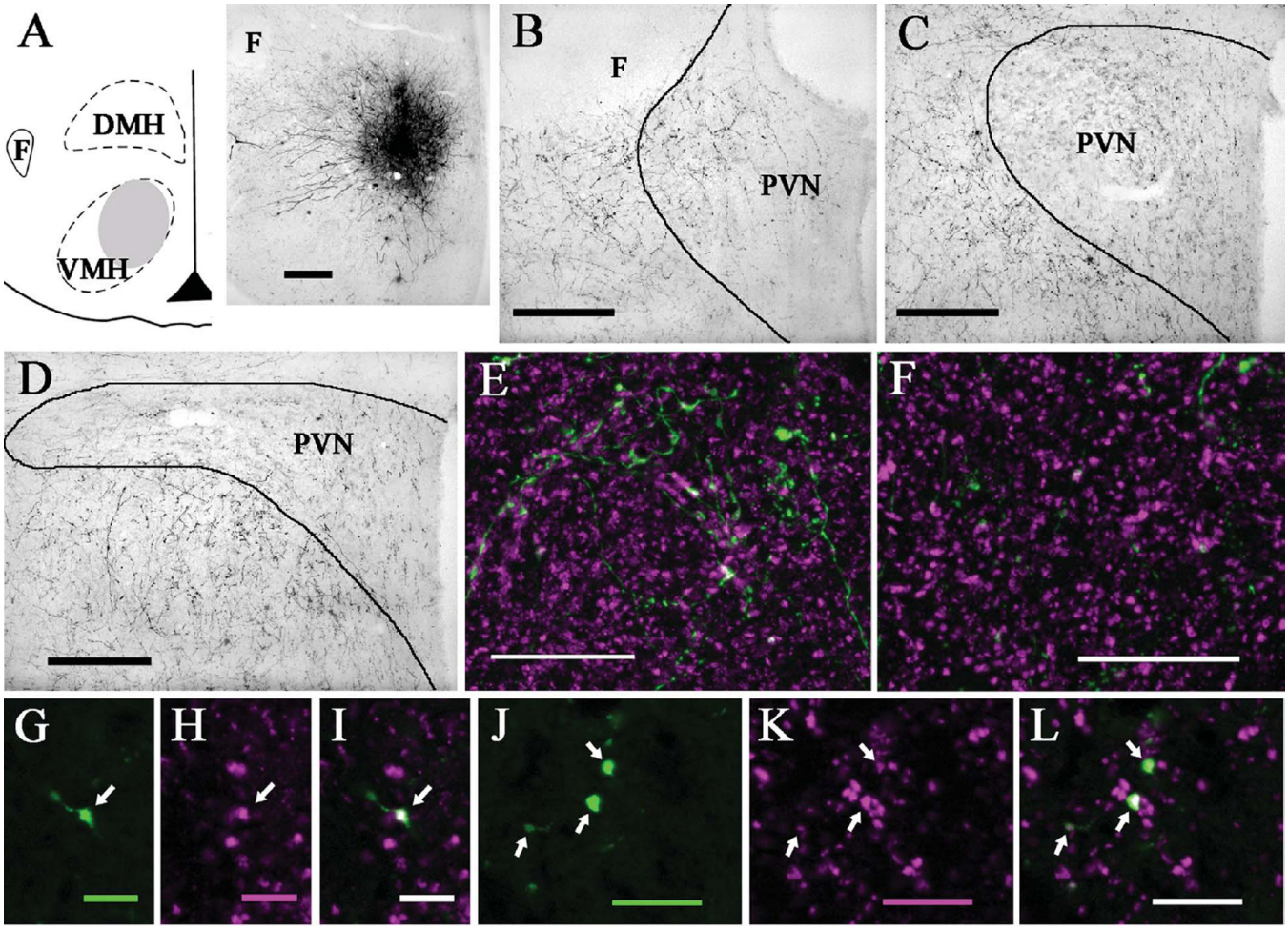

Figure 4.

PhaL injections into the ventromedial hypothalamic nucleus produced more anterogradely labeled fibers in the anterior than posterior PVN. **A**: Diagram (left) and brightfield image (right) depicting the location of a PhaL injection site in the ventromedial nucleus (case 15; ≈bregma −2.8 mm). **B**: Brightfield image shows numerous PhaL-positive fibers and boutons in the anterior PVN (≈bregma −0.8 mm) and its surround. **C**: At the level of mid PVN (≈bregma −1.8 mm), few PhaL fibers and boutons are seen in the parvocellular subdivision with even less in the magnocellular subdivision; some PhaL-positive fibers occur in the PVN surround. **D**: In the posterior PVN (≈bregma −2.1 mm), there are few PhaL-positive fibers and boutons in the medial portion and even fewer in the lateral portion, with numerous PhaL-positive fibers occurring ventrally in the PVN surround (i.e., sub-PVN). Dual immunolabeling for PhaL (green) and VGluT2 (magenta) shows a greater density of PhaL-positive fibers and boutons in anterior (**E**) versus posterior (**F**) PVN, with relatively comparable levels of VGluT2 labeling (images are projections made from z-stack images). In the anterior PVN, higher magnification views of a single optical section (≈0.45 μm thick) show a PhaL-positive bouton (arrow; **G**) that is also positive for VGluT2 (arrow; **H,I**; dual labeling appears white). In the posterior PVN, higher magnification views of a single optical section (≈0.45 μm thick) show three PhaL-positive boutons (arrows; J) that are also positive for VGluT2 (arrows; **K,L**). Diagram in (A) modified from Paxinos and Watson (1998). Scale bars = 200 μm for A–D; 20 μm for E,F; 5 μm for G–I; 10 μm for J–L.

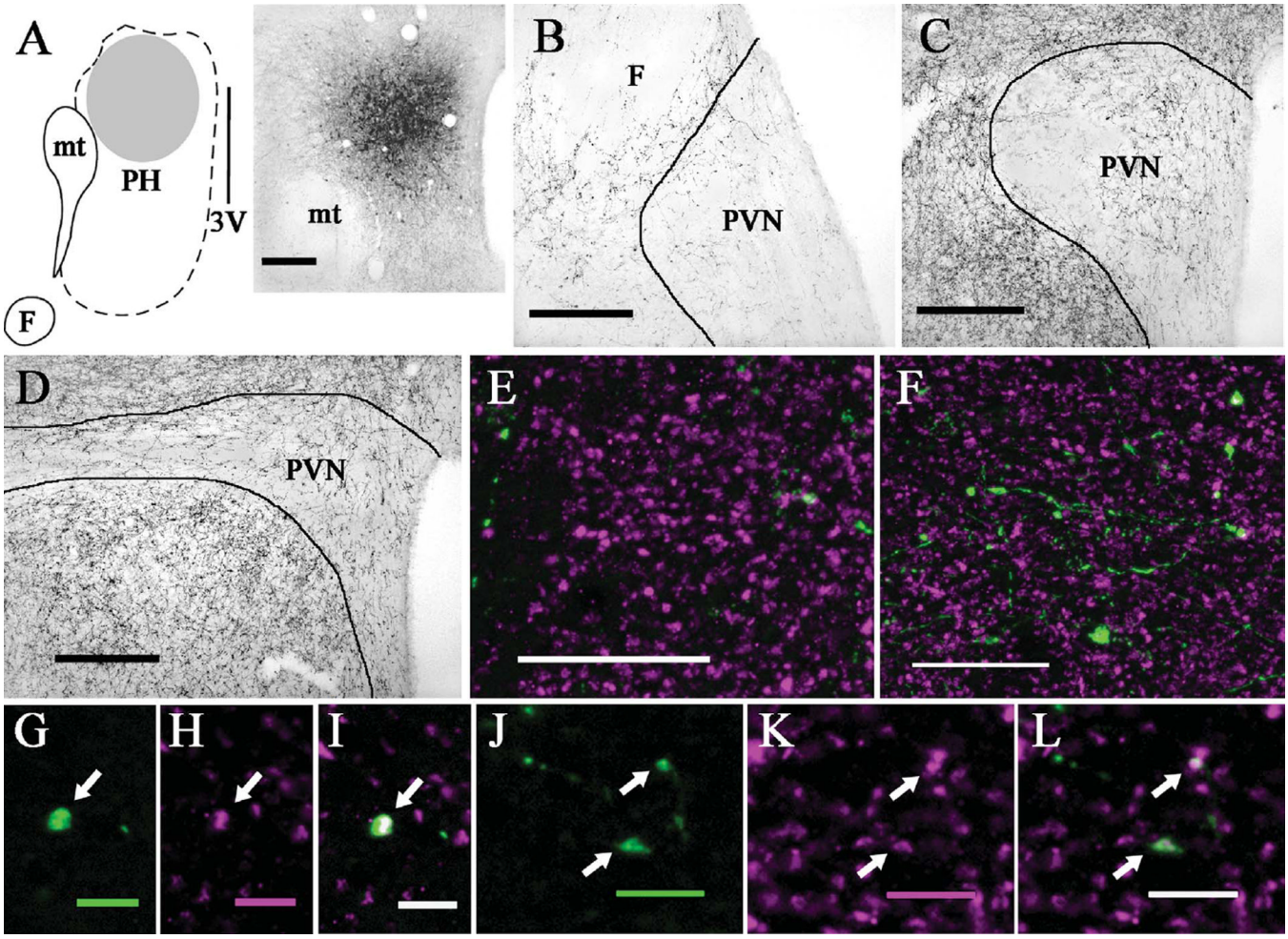

Figure 5.

PhaL injections into the posterior hypothalamic nucleus produced more anterogradely labeled fibers in the posterior than anterior PVN. **A**: Diagram (left) and brightfield image (right) depicting the location of a PhaL injection site in the posterior nucleus (case 8; ≈bregma −3.8 mm). **B**: Brightfield image shows few PhaL-positive fibers and boutons in the anterior PVN (≈bregma −0.8 mm). **C**: At the evel of mid PVN (≈bregma −1.8 mm), many PhaL fibers and boutons are seen in the parvocellular subdivision with less in the magnocelular subdivision; the greatest density of PhaL-positive fibers occurs in the PVN surround. **D**: In the posterior PVN (≈bregma −2.1 mm), there are numerous PhaL-positive fibers and boutons throughout the PVN and an even greater fiber density in the PVN surround. Dual immunolabeling for PhaL (green) and VGluT2 (magenta) shows a lower density of PhaL-positive fibers and boutons in anterior (**E**) versus posterior (**F**) PVN, with relatively comparable levels of VGluT2 labeling (images are projections made from z-stack images). In the anterior PVN, higher magnification views of a single optical section (≈0.45 μ.m thick) show a rare PhaL-positive bouton (arrow; **G**) that is also positive for VGluT2 (arrow; **H,I**). In the posterior PVN, higher magnification views of a single optical section (≈0.45 μm thick) show two PhaLpositive boutons (arrows; **J**) that are also positive for VGluT2 (arrows; **K,L**; dual labeling appears white); dual-labeled boutons are much more commonly observed in the posterior versus anterior PVN. Diagram in (A) modified from Paxinos and Watson (1998). Scale bars = 200 μm for A–D; 20 μm for E,F; 5 μm for G–L.

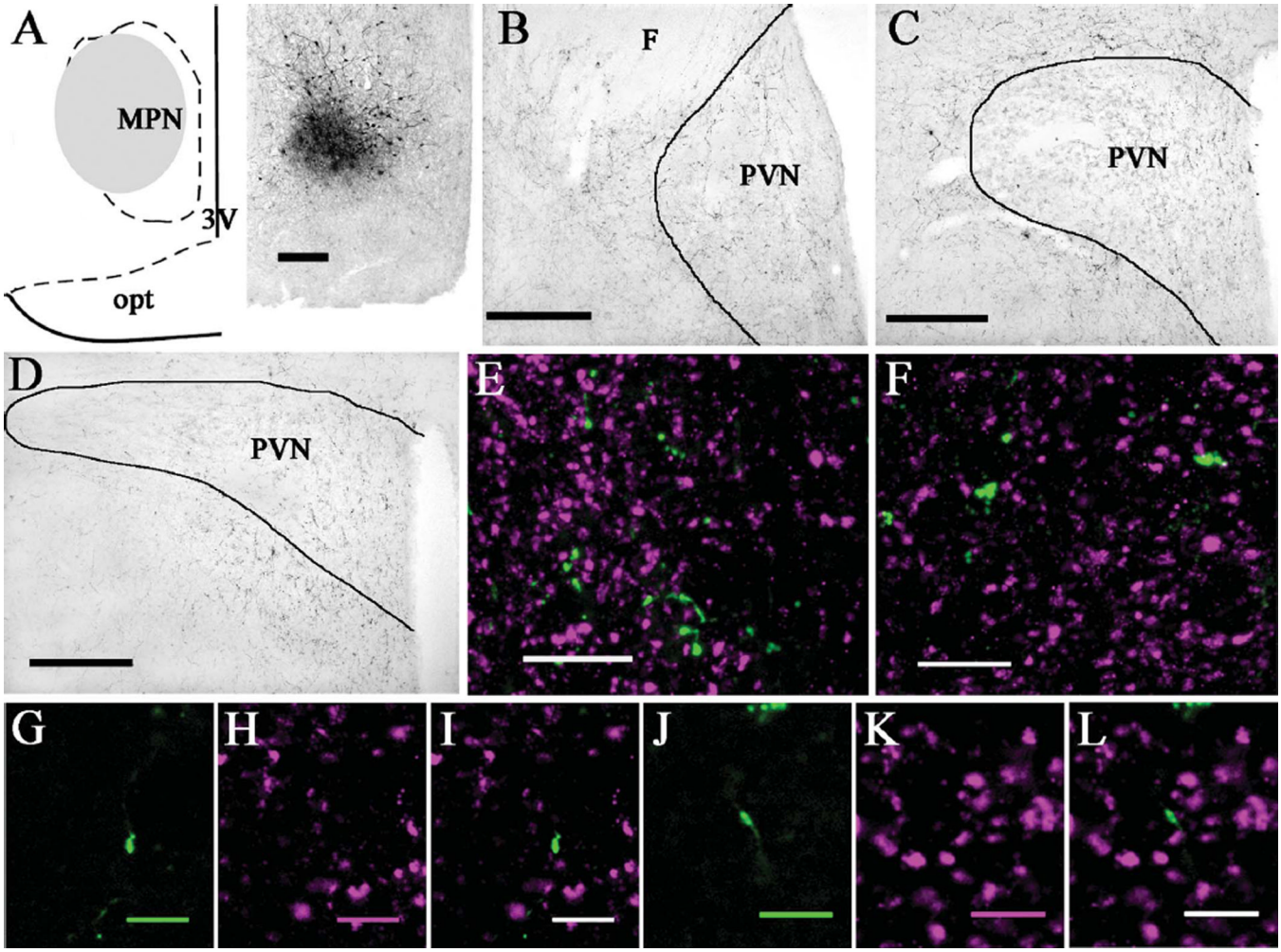

Figure 6.

PhaL injections into the medial preoptic hypothalamic nucleus produced more anterogradely labeled fibers in the anterior than posterior PVN. **A**: Diagram (left) and brightfield image (right) depicting the location of a PhaL injection site in the medial preoptic nucleus (case 20; ≈bregma −0.8 mm). **B**: Brightfield image shows numerous PhaL-positive fibers and boutons in the anterior PVN (≈bregma −0.8 mm) and its surround. **C**: At the level of mid PVN (≈bregma −1.8 mm), few PhaL fibers and boutons are seen in the parvocellular subdivision with even less in the magnocellular subdivision; some PhaL-positive fibers occur in the PVN surround. **D**: In the posterior PVN (≈bregma −2.1 mm), there are few PhaL-positive fibers and boutons in the medial portion and even fewer in the lateral portion, with some PhaL-positive fibers occurring in the PVN surround. Dual immunolabeling for PhaL (green) and VGluT2 (magenta) shows a greater density of PhaL-positive fibers and boutons in anterior (**E**) versus posterior (**F**) PVN, with relatively comparable levels of VGluT2 labeling (images are projections made from z-stack images). In the anterior PVN, higher magnification views of a single optical section (≈0.48 μm thick) show a PhaL-positive bouton (**G**) that is not positive for VGluT2 (**H,I**). In the posterior PVN, higher magnification views of a single optical section (≈0.41 μm thick) show a PhaL-positive bouton (**J**) that is not positive for VGluT2 (**K,L**); dual labeled boutons were not observed in either the anterior or posterior PVN. Diagram in (A) modified from Paxinos and Watson (1998). Scale bars = 200 μm for A–D; 10 μm for E,F; 5 μm for G–L.

TABLE 1

Primary Antibodies Used

Antigen	Immunogen	Manufacturer, species, type, catalog number	Dilution used
Fluorogold	Fluorogold	Stanley Watson, rabbit polyclonal antisera	1:5,000
PhaL	*Phaseolus vulgaris* agglutinin (E+L)	Vector Laboratories, goat affinity purified polyclonal antisera, #AS-2224	1:3,000
VGluT2	Strep-Tag fusion protein containing amino acid residues 510–582 of rat VGluT2	Synaptic Systems, rabbit polyclonal antisera, #135–402	1:500

TABLE 2

Ipsilateral VGluT2-positive projections to the anterior versus posterior PVN and its surround. Values are shown for each individual anterior-to-mid (90, 110, and 112) and posterior-to-mid (102, 104, and 109) PVN case, as well as for the mean of each group

	Case 90		Case 110		Case 112		Case 102		Case 104		Case 109		Anterior Cases (Mean ± SEM)		Posterior Cases (Mean ± SEM)	
	#FG	%	#FG	%	#FG	%	#FG	%	#FG	%	#FG	%	#FG	%	#FG	%
BST																
BSTad	34	0	25	0	15	0	0	0	5	0	12	0	25 ± 7	0±0	6±4	0±0
BSTav	34	0	17	0	16	0	37	14	11	0	12	0	22 ± 7	0±0	20 ± 10	5±6
BSTif/v	99	0	14	0	14	0	4	25	40	13	17	18	42 ± 35	0±0	20 ± 13	18 ± 4
BSTpr	24	0	18	0	7	0	6	0	8	25	9	22	16 ± 6	0±0	8±1	16 ± 10
Hypothalamus																
AHA	65	0	62	2	21	0	0	0	5	0	14	21	49 ± 17	1±1	6±5	7±9
AHNa	30	3	17	12	17	18	35	37	14	43	5	0	21 ± 5	11 ± 5	18 ± 11	27 ± 16
AHNc	149	4	68	6	39	15	23	39	77	22	58	5	85 ± 40	8±4	53 ± 19	22 ± 12
AHNp	11	0	7	0	14	0	15	13	11	0	7	14	11 ± 2	0±0	11 ± 3	9±6
ARC	6	0	18	6	25	0	3	67	2	0	3	0	16 ± 7	2±2	3±0	22 ± 27
DMHa	16	0	5	0	17	6	36	31	11	45	11	9	13 ± 5	2±2	19 ± 10	28 ± 13
DMHp	7	0	4	0	4	0	16	38	0	0	4	0	5±1	0±0	7±6	13 ± 15
DMHv	0	0	4	0	11	27	6	50	5	100	9	67	5±4	9 ± 11	7±1	72 ± 18
LHA	310	0	104	6	101	6	167	28	164	31	128	22	172 ± 85	4±2	153 ± 15	27 ± 3
LPO	13	8	12	8	1	0	13	8	30	17	28	7	9±5	5±3	24 ± 7	11 ± 4
MePO	25	8	1	0	4	0	1	100	7	43	11	18	10 ± 9	3±3	6±4	54 ± 30
MPO	96	0	44	0	35	0	59	8	15	20	28	18	58 ± 23	0±0	34 ± 16	15 ± 4
MPN	111	1	90	1	96	15	19	26	8	13	34	3	99 ± 8	6±6	20 ± 9	14 ± 8
PH	30	0	16	0	11	0	45	49	34	74	95	58	19 ± 7	0±0	58 ± 23	60 ± 9
PM	na		na		na		na		na		18	89	na		18†	89†
PV	22	0	9	0	9	0	0	0	2	0	3	33	13 ± 5	0±0	2±1	11 ± 14
RCH	19	0	25	0	11	0	8	0	8	25	6	0	18 ± 5	0±0	7±1	8 ± 10
SCH	9	0	41	0	10	0	0	0	0	0	14	14	20 ± 13	0±0	5±6	5±6
Tub	10	0	16	6	15	0	8	25	6	0	5	40	14 ± 2	2±3	6±1	22 ± 14
VMHc	65	18	30	40	21	10	16	81	22	91	15	60	39 ± 16	23 ± 11	18 ± 3	77 ± 11

	Case 90		Case 110		Case 112		Case 102		Case 104		Case 109		Anterior Cases (Mean ± SEM)		Posterior Cases (Mean ± SEM)	
	#FG	%	#FG	%	#FG	%	#FG	%	#FG	%	#FG	%	#FG	%	#FG	%
VMHdm	61	13	32	44	23	26	29	72	18	72	36	81	39 ± 14	28 ± 11	28 ± 6	75 ± 4
VMHvl	35	20	46	30	17	29	24	71	19	95	6	100	33 ± 10	27 ± 4	16 ± 7	89 ± 11
Other sites																
MeA	148	1	41	10	36	0	5	80	47	47	28	29	75 ± 45	3±4	27 ± 15	52 ± 18
LS	5	0	24	0	na		na		58	0	142	0	15†	0†	100†	0†
PVT	18	28	2	0	13	0	8	100	18	72	45	73	11 ± 6	9 ± 11	24 ± 14	82 ± 11
SI	13	0	11	0	4	0	9	11	47	21	32	16	9±3	0±0	29 ± 14	16 ± 4
ZI	126	1	1	0	8	0	49	0	102	3	87	5	45 ± 50	0±0	79 ± 19	3±2

#FG denotes the number of FG-positive cell bodies observed in each forebrain region. % denotes the percentage of these FG-positive cell bodies that co-expressed VGluT2 mRNA. na denotes not available.

† denotes that the n was insufficient to permit calculation of the SEM.

TABLE 3

Abbreviations Used in Figures and Tables

AAA	anterior amygdaloid area	MPN	medial preoptic nucleus
ac	anterior commissure	mt	mammillothalamic tract
ADP	anterodorsal preoptic nucleus	och	optic chiasm
AHA	anterior hypothalamic area	opt	optic tract
AHNa	anterior hypothalamic nucleus, anterior part	PaAP	paraventricular hypothalamic nucleus, anterior parvicellular
AHNc	anterior hypothalamic nucleus, central part	PaMP	paraventricular hypothalamic nucleus, medial parvicellular
AHNp	anterior hypothalamic nucleus, posterior part	PaPo	paraventricular hypothalamic nucleus, posterior
ARC	arcuate hypothalamic nucleus	PH	posterior hypothalamic nucleus
AVP	anteroventral preoptic nucleus	PM	premammillary nucleus
BMA	basomedial amygdaloid nucleus	PT	parataenial thalamic nucleus
BSTad	bed nucleus of the stria terminalis, anterodorsal	PV	periventricular hypothalamic nucleus
BSTav	bed nucleus of the stria terminalis, anteroventral	PVN	paraventricular hypothalamic nucleus
BSTif/v	bed nucleus of the stria terminalis, interfascicular and ventral	PVT	paraventricular thalamic nucleus
BSTpr	bed nucleus of the stria terminalis, principle	RCH	retrochiasmatic area
cc	corpus callosum	Re	reuniens thalamic nucleus
CeA	central amygdaloid nucleus	RT	reticular thalamic nucleus
DMH	dorsomedial hypothalamic nucleus	SCH	suprachiasmatic nucleus
DMHa	dorsomedial hypothalamic nucleus, anterior	SI	substantia innominata
DMHp	dorsomedial hypothalamic nucleus, posterior	SM	stria medullaris
DMHv	dorsomedial hypothalamic nucleus, ventral	3V	third ventricle
F	fornix	Tub	tuberal nucleus
int	internal capsule	VM	ventromedial thalamic nucleus
LHA	lateral hypothalamic area	VMH	ventromedial hypothalamic nucleus
LPO	lateral proptic area	VMHa	ventromedial hypothalamic nucleus, anterior part
LS	lateral septum	VMHc	ventromedial hypothalamic nucleus, central part
MA	magnocellular preoptic nucleus	VMHdm	ventromedial hypothalamic nucleus, dorsomedial part
MeA	medial amygdaloid nucleus	VMHvl	ventromedial hypothalamic nucleus, ventolateral part
MePO	median preoptic nucleus	VRe	reuniens thalamic nucleus, ventral part
MPO	medial preoptic area	ZI	zona incerta